약학박사학위논문

고지혈 환경에서
자가 항체 반응 조절에 대한 연구

Regulation of Autoantibody Responses in Hyperlipidemia

2019 년 8 월

서울대학교 대학원

약학과 의약생명과학 전공

류 희 주

고지혈 환경에서
자가 항체 반응 조절에 대한 연구

Regulation of Autoantibody Responses in Hyperlipidemia

지도교수 정 연 석

이 논문을 약학박사 학위논문으로 제출함

2019 년 5 월

서울대학교 대학원
약학과 의약생명과학 전공

류 희 주

류희주의 박사학위논문을 인준함

2019 년 6 월

위 원 장	강 창 율	(인)
부 위 원 장	이 미 옥	(인)
위 원	윤 지 희	(인)
위 원	최 윤 수	(인)
위 원	정 연 석	(인)

ABSTRACT

Regulation of Autoantibody Responses in Hyperlipidemia

Heeju Ryu
College of Pharmacy
Department of Pharmacy Graduate School
Advisor: Prof. Yeonseok Chung

Systemic lupus erythematosus (SLE) is an antibody-mediated autoimmune disease that exhibits abnormal activation of immune systems, which leads failure of multiple organs. Meanwhile, atherosclerosis is a chronic inflammatory disease that caused by accumulation of fatty materials in inner artery and alteration in lipid metabolism. Patients with SLE exhibited higher incidence of atherosclerosis. However, despite of the tight associated between proatherogenic factors and immune systems, the contribution of hyperlipidemic conditions to immune responses, particularly antibody-mediated humoral responses, remains unclear. In this study, I propose a novel mechanism by which alteration in lipid metabolism regulates germinal center reactions and consequent antibody production.

Atherosclerosis-prone *Apoe*$^{-/-}$ and *Ldlr*$^{-/-}$ mice reconstituted with lupus-prone BXD2 bone marrow showed exacerbated glomerulonephritis phenotypes and autoantibody production, particular increase in pathogenic IgG2c isotype. Alteration in lipid metabolism by feeding high-fat diet also enhanced theses phenomena. The severity of disease and antibody production were strongly associated with increased follicular helper T cells (T_{FH} cells). T_{FH} cells isolated from *Apoe*$^{-/-}$ mice had higher expression of genes associated with inflammatory responses and SLE, and were more potent in inducing IgG2c production. Among T_{FH} cell subsets, CXCR3-expressing T_{FH} cells are susceptible to promote IgG2c in IFN-γ-dependent manner.

Mechanistically, the atherogenic environment and proatherogenic factor, oxidized low-density lipoprotein (oxLDL), induced IL-27 from dendritic cells (DCs), particularly in $CD11b^+$ DCs. Alteration in lipid metabolism and Liver X receptor (LXR) expression regulated IL-27 production by atherogenic DCs. Deletion of Toll-like receptor 4 (TLR4) diminished IL-27 production as well as antibody-generating germinal center reactions.

IL-27 stimulated STAT1 and STAT3 signaling pathway in T_{FH} cells to increase the numbers of $CXCR3^+$ T_{FH} cells while suppressing follicular regulatory T cells (T_{FR} cells). Blockade of IL-27 signals diminished the increased T_{FH} responses in atherogenic mice. Patients with hypercholesterolemia exhibited elevated levels of IL-27 as well as IgG1 and IgG3 antibodies in circulation, which is in a good agreement with the findings in animal models. Thus 'hyperlipidemia–TLR4/LXR–IL-27–$CXCR3^+$ T_{FH} cell' axis might explain the tight association between atherosclerosis and SLE in humans, can be a potential therapeutic target for atherosclerosis-related autoimmune diseases.

Key words: hyperlipidemia, autoimmune diseases, follicular helper T cell, germinal center reaction, interleukin-(IL-)27

Student Number: 2014-22972

CONTENTS

LIST OF TABLES

LIST OF FIGURES

LIST OF ABBREVIATIONS

SLE: Systemic Lupus Erythematosus

T_{FH} cell: Follicular helper T cell

oxLDL: Oxidized low-density lipoprotein

TLR4: Toll-like receptor 4

APC: Antigen-presenting cell

DC: Dendritic cell

T_H: Helper T cell

T_{REG} cell: Regulatory T cells

fDC: Follicular dendritic cell

GC: Germinal center

GC B: Germinal center B cell

IFN: Interferon

NET: Neutrophil extracellular trap

LXR: Liver X receptor

PPAR: Peroxisome proliferator- associated receptor

RXR: Retinoid X receptor

RAR: Retinoic acid receptor

HFD: High-fat diet

KLH: Keyhole limpet hemocyanin

NP: 4-hydroxy-3-nitrophenyl

T_{FR} cell: Follicular regulatory T cell

PC: Plasma cell

PAMP: Pathogen-associated molecular pattern

IL: Interleukin

I. Introduction

1. Helper T cell diversity and germinal center reaction

1.1 Helper T cell diversity

The immune system defends our body against foreign antigens such as bacteria, viruses, or parasite, and even forms a memory to eliminate second invasion effectively. Upon antigen stimulation by antigen-presenting cells (APCs) such as dendritic cells (DCs), naive $CD4^+$ T cells can be activated and further differentiated into specialized effector cell population, called helper T (T_H) cells, which serve distinct immunological roles. Helper T cells can be subcategorized into at least 5 different subsets based on their cytokine production and transcription factors. T_H1 cells are characterized by IFN-γ production and T-BET expression whose differentiation depends on IL-12 production by DC. They activate macrophages and generate immune responses against microbes and internal parasites. T_H2 cells secrete IL-4, IL-5 and IL-13 with GATA3 transcription factor expression. They defense against external parasites. IL-6, TGFβ, IL-23 and IL-1β stimulation leads RORγt-expressing T_H17 cell differentiation, which secrete IL-17A, IL-17F and IL-22 to mediate mucosal immunity against extracellular bacteria. Regulatory T (T_{REG}) cells, which can be differentiated by TGFβ, secrete TGF-β and IL-10 and express Foxp3 as transcription factor, mediate immune tolerance and monitor proper immune responses. A new T_H subset, called follicular helper T (T_{FH}) cells, is differentiated by IL-21, IL-6, IL-12 and IL-27 cytokine stimulation, and secrete IL-21, IL-4, and/or IFN-γ cytokines to provide B cell help (**Figure 1**). Other subsets, such as T_H9 (secretes IL-9) and T_H22 (produces IL-22) are also suggested[1].

1.2 Follicular helper T cell

Follicular helper T (T_{FH}) cells are characterized by surface expression of CXC-chemokine receptor 5 (CXCR5), inducible T cell co-stimulator (ICOS), and programmed cell death protein 1 (PD-1), and by transcription factor expression of B-cell lymphoma 6 protein (BCL6) and Achaete-scute homolog 2 (ASCL2). Some studies suggested that T_{FH} cells can subdivided into 3 different subsets based on their surface expression of CXCR3 and CCR6: $CXCR3^+CCR6^-$ (sometimes called as $T_{FH}1$), $CXCR3^-CCR6^+$ ($T_{FH}2$), and $CXCR3^-CCR6^+$ ($T_{FH}17$)[2]. $CXCR3^+CCR6^-$ TFH cells are characterized by IFN-g production and T-BET expression, while $CXCR3^-CCR6^+$ or $CXCR3^-CCR6^+$ TFH cells

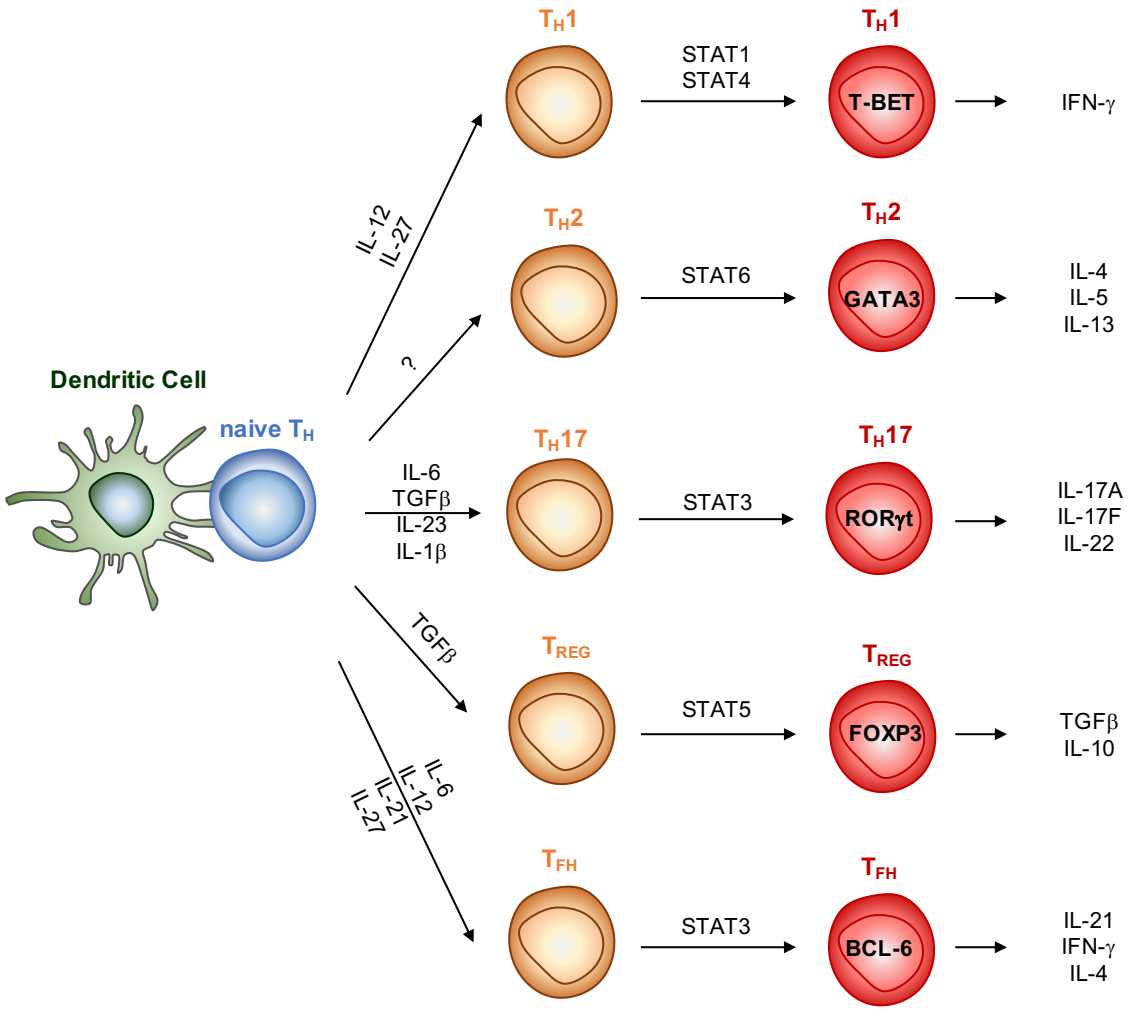

Figure 1. *Helper T cell differentiation*

Upon stimulation by dendritic cells, naive $CD4^+$ T cells can be activated and differentiated into effector helper T cells.

secrete IL-4/5/13 or IL-17A and IL-22, respectively[2, 3]. Along with IL-21, T_{FH} cells produce IFN-γ and IL-4 for class switching of IgG2a/c and IgG1, respectively, during T-B interaction[4]. However, explicit mechanism by which T_{FH} cells and their subsets are differentiated is not clear. Most plausible mechanism, so far, is that T_{FH} cell differentiation is multistage and multifactorial integrated model with initiation, maintenance/commitment and full polarization, which requires multiple signals from other cells (**Figure 2**). Also, transcription factor STAT3, c-Maf, Batf, and IRF4 are involved in controlling function of T_{FH} cells[4].

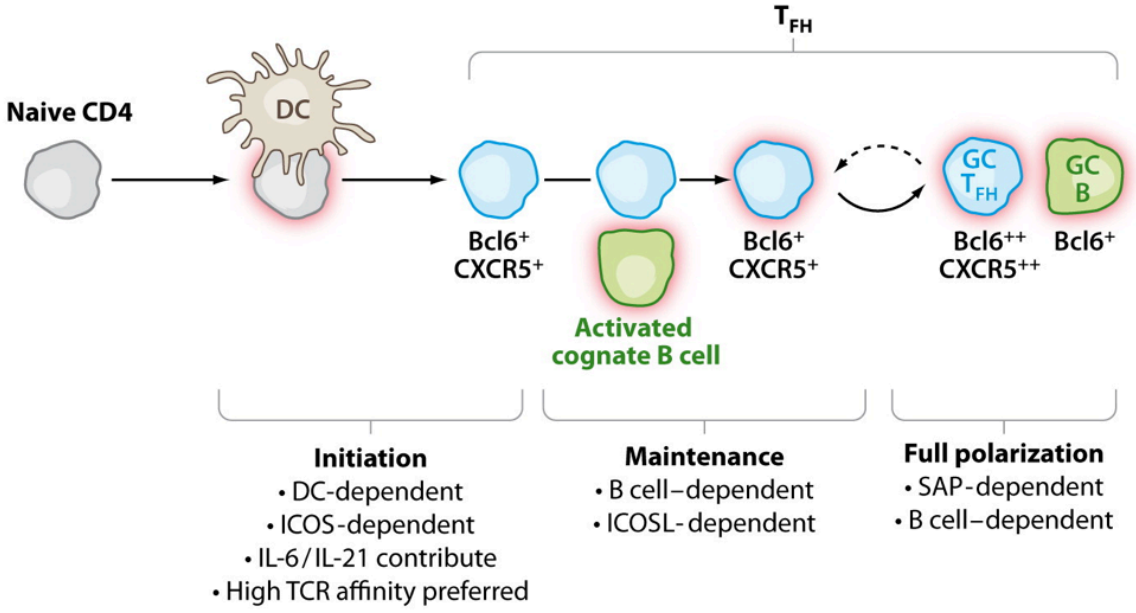

Figure 2. *Model of T_{FH} cell differentiation*[3]

Multiple stages are involved for T_{FH} cell differentiation, including initiation, maintenance, and full polarization.

1.3 Germinal center reaction

Germinal center reaction is a series of process that B cells become diversified and matured to form high affinity antibodies. When naive T cells are activated by antigen stimulation by APCs, they express CXCR5 on their surface to migrate into T cell-B cell border in secondary lymphoid organs. Resting B cells also move to T-B border after acquisition of antigen, and receive co-stimulatory signals from activated T cells, called linked recognition. This process triggers activation of B cells and differentiation of T_{FH} cells. Some activated B cells turn into short-lived plasmablast that secreted low-affinity antibodies. Others move into the center of B cell follicles together with T_{FH} cells and follicular DCs (fDCs), and proliferate to form early germinal centers. After massive expansion, B cells undergo somatic hypermutation to become diversified, are selected by T_{FH} cells and fDCs to improve their binding ability to the antigen, and experience immunoglobulin (Ig) class-switch recombination to acquire different isotypes. After several rounds of mutation and selection, germinal center B (GC B) cells are differentiated into high-affinity-antibody-secreting plasma cells or memory B cells and

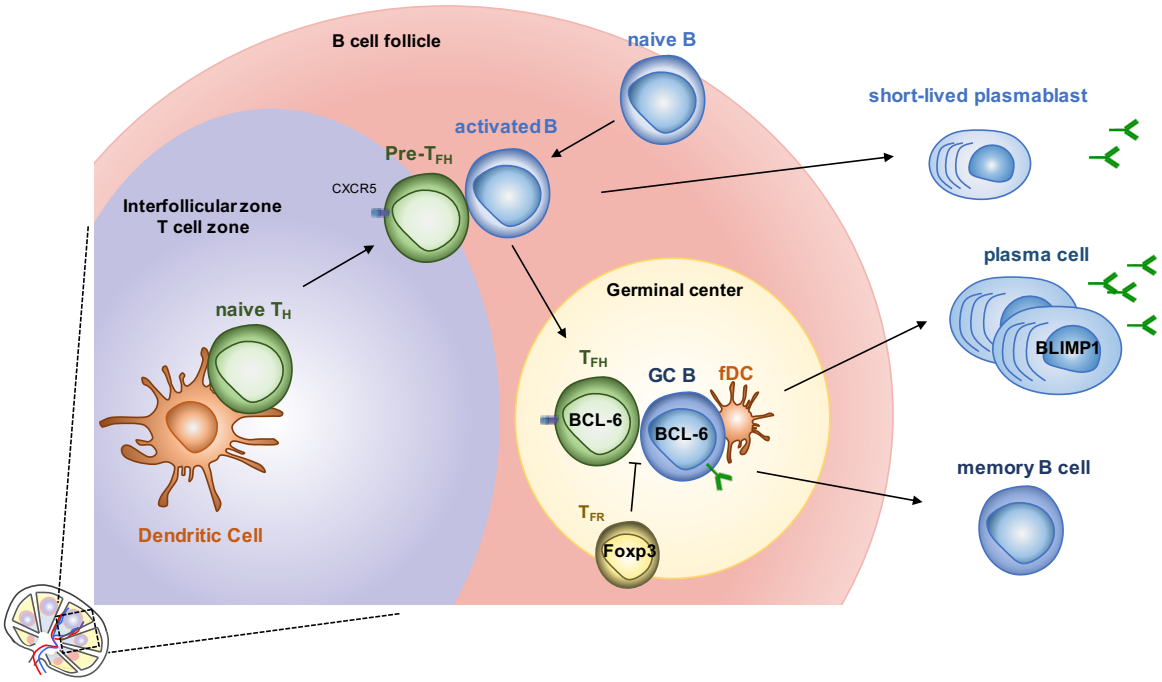

Figure 3. *Dynamics of germinal center reactions*

Germinal center reactions occur in secondary lymphoid organs. Pre-T_{FH} and activated B cells are differentiated into T_{FH}, and GC B cells, respectively. GC B cells can be further differentiated into antibody-secreting plasma cell or memory B cells.

finally exit germinal centers. Recently, a new subset of T_{REG} cells, called follicular regulatory T (T_{FR}) cells, expressing CXCR5 and BCL6, is discovered, and they reside in the germinal center to suppress the function of T_{FH} cells and GC B cells (**Figure 3**)[5].

While sufficient helper T cell responses or germinal center reactions lead adequate host defense against foreign antigens, aberrant T cells and B cells activities raise other side effects, such as autoimmunity[1].

2. Systemic lupus erythematosus

Systemic lupus erythematosus (SLE) is an antibody-mediated autoimmune disease, which leads significant damage in multiple organs by their own immune system. The reported prevalence of SLE is 0.2-2 per 1,000 (2-4 per 1,000 for women) world-widely[6]. Since the heterogeneity of the diseases, the diagnosis of SLE based on various characteristic clinical findings of the skin, kidney, joints, and central nervous system, as well as on serological parameters including high levels of autoantibodies such as anti-

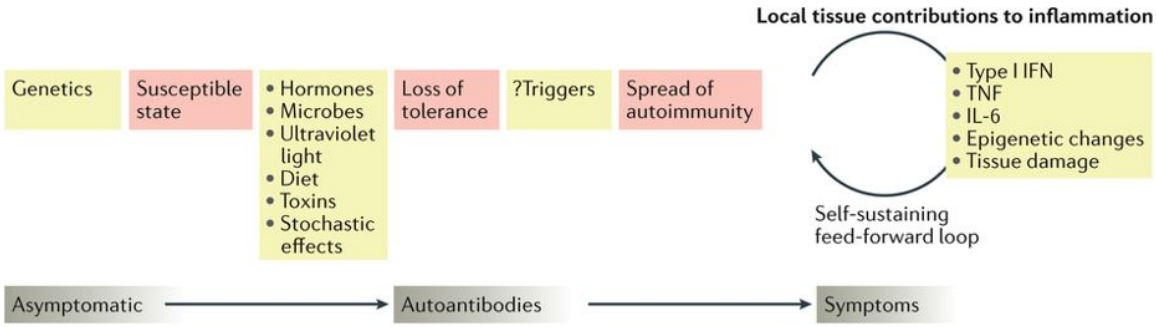

Figure 4. *Schematic diagrams of pathogenesis of systemic lupus erythematosus*[7]

The progression of systemic lupus erythematosus (SLE) includes various symptoms and discrete stages. Environmental and genetic factors contribute to the development of disease, but the elements that drive a spreading of autoimmunity are poorly understood. Immune-complex deposition, cytokines and autoantibody-mediated tissue damage can drive irreversible damage in various organs.

dsDNA, anti-histone, anti-Ro, anti-La, and rheumatoid factor. These various clinical symptoms do not occur simultaneously and may develop at any stage of the disease. More than 60 genes are proposed as a risk allele for causation of SLE, but no clear mechanism has been suggested by which SLE is progressed[7].

Aberrant innate immune responses play a significant role in the pathogenesis of SLE, contributing both to tissue injury via release of inflammatory cytokines as well as to activation of autoreactive T and B cells. Type I interferons (IFNs), IL-6, and IL-10 cytokines produced by dendritic cells are strongly associated with autoantibody titers in patients with SLE and blockade of these cytokines can be used for therapeutic strategy. Also, neutrophil extracellular trap (NET) DNA, generated by NETosis, can be used for autoantigen for DC, and activate autoreactive T cell[7].

Activation of autoreactive T and B cells lead to pathogenic autoantibody production and organ injury as a resultant. Given that plasma cells (PCs) are responsible for the generation of these pathogenic antibodies, a number of studies have been done to analyze the function of autoreactive B cells and T cells. Number of activated B cells producing Ig is increased in peripheral blood with more prone polyclonal activation by antigens. Increased secretion of type 1 interferons (IFN-α), IL-6, and IL-10, mainly secreted by DCs, amplify B cell hypersensitivity by enhancing B cell proliferation and differentiation. Defects in self-tolerance with enhanced BCR, TLR and BAFF receptor

signaling promotes survival of autoreactive B cells, which in turns leads differentiation of pathogenic memory and plasma cells via autoreactive germinal center reaction. Also, increased numbers of hyperactivated T cells, especially T_{FH} cells, are increased in lupus patients with skewing towards B cell help and Ig production (**Figure 4**)[8].

Numerous immunotherapeutic strategies for the treatment of SLE have been suggested, particularly targeting B cells (**Table 1**). Surprisingly, these clinical trials rarely reach the ultimate cure of the disease, rather alleviate the symptoms, suggesting that alternative therapeutic strategies should be considered[9].

Table 1. List of current SLE therapies in clinical trials[8]

Molecular target	Treatment	Status
B CELLS		
BAFF/APRIL	Belimumab	Approved for non-renal SLE Ongoing phase IV for efficacy, safety, and tolerability Ongoing phase III in combination with Rituximab
	Tabalumab	Phase III without significant effect (terminated)
	Blisibimod	Phase III did not meet SRI-6 primary end point
	Atacicept	APRIL-SLE study terminated due to increased infection rate ADDRESS II study has acceptable safety profile
CD20	Rituximab	Phase III failed (nephritis and non-nephritis)
	Ocrelizumab	Phase III trial completed
CD22	Epratuzumab	Phase III failed
CD19	XmAb5871	Phase II trial
Proteasome inhibitors	Bortezomib	Phase II trial
INTRACELLULAR SIGNALING		
Btk	M2951	Ongoing phase II
	Fenebrutinib	Ongoing phase II trial
mTOR	N-acetylcysteine	Small study showed decrease in SLEDAI, no further development
	Rapamycin	Open-label study showed an effect on BILAG. Larger study planned.
JAK/STAT	GSK2586184	Ineffective on interferon signature in phase II, safety data do not support further study
JAK 2	Baricitinib	Phase II positive data; Phase III trial ongoing
JAK3	Tofacitinib	Ongoing Phase I/II trial
ROCK	Fasudil	Effective in preclinical studies in patient with Raynaud's, phase III completed with uninterpretable data.

Molecular target	Treatment	Status
CO-STIMULATION		
CD40:CD154	Dapirolizumab	Ongoing phase II trial
	BI 655064	Ongoing phase II trial
CD28:B7	Abatacept	Ineffective in phase III in nephritis and general SLE
	Lulizumab	Phase II trial terminated—failed to meet protocol objectives
CYTOKINES		
	Sifalimumab	Limited effect in phase II and III. No further development
	Rontalizumab	Phase II without significant results
Interferon-α	Anifrolumab	Phase II positive data; 2 Phase III trials ongoing (one reported negative)
	IAGS-009	Completed phase I, no data released
	JNJ-55920839	In recruiting phase
	IFNα-k	Successful phase I; ongoing phase II trial
Interleukin-2	Aldesleukin	Ongoing open-label phase II trial
	AMG 592	Ongoing phase Ib and IIa trial
	ILT-101	Ongoing phase II trial
Interleukin 12/23	Ustekinumab	Met primary end-point in phase II trial; ongoing phase III trial
Interleukin-6	PF-04236921	Failed phase II trial; safety compromised
	Sirukumab	Failed phase II trial
	MRA003US	Ongoing phase II trial
	Vobarilizumab	Ongoing phase I trial
Interleukin-10	BT063	Ongoing phase II trial
OTHER		
	Lupuzor	Phase III trial failed to meet the primary end point

3. Atherosclerosis and autoimmunity

Atherosclerosis is a chronic inflammatory disease within the subendothelial area of the artery, and is one of the leading causes of death worldwide. In addition to a critical role of hyperlipidemia in the atherogenesis, it is well-demonstrated that both innate and adaptive immune cells contribute to the development of atherosclerosis. For instance, there is an intense accumulation of macrophages and T cells in the atherosclerotic lesions in animal models and in humans. Macrophages and dendritic cells recognize fatty materials such as long-chain saturated fatty acids and modified LDL through scavenger receptors or Toll-like receptors (TLRs), and secrete inflammatory cytokines and chemokines, aggravating vascular inflammation. In addition, T_H1 and T_H17 cells are found in the lesion, and T_H1 cells appear to be pro-atherogenic while the role of T_H17 cells remains controversial. By contrast, there is increasing evidence that particular subsets of T cells including Foxp3-expressing T_{REG} and T_H2 cells inhibit the development of this vascular disease in animal models. Thus, different types of immune cells play either pathogenic or protective roles in atherosclerosis.

Of interest, patients with systemic autoimmune disorders show an increased incidence of atherosclerosis; these atherosclerosis-related autoimmune diseases include psoriasis, rheumatoid arthritis (RA), and systemic lupus erythematosus (SLE), all of which are known to be mediated by autoreactive T cells (**Table 2**)[10, 11, 12, 13, 14]. Among the atherosclerosis-related autoimmune diseases, SLE and RA are thought to be mediated T_{FH} cell and consequent autoantibody production[15]. Dyslipidemia also found in patients with SLE, and normalizing the levels of glycosphingolipids restores the function of $CD4^+$ T cells to decrease the levels of anti-dsDNA autoantibodies in lupus patients[16]. The disease activity of SLE, including the SLE disease activity index (SLEDAI) and the levels of anti-double stranded DNA (dsDNA), is positively associated with the level of

Table 2. List of atherosclerosis-related autoimmune diseases

Index of correlation	Relevant autoimmune diseases
increased incidence rate of atherosclerosis	rheumatoid arthritis, systemic lupus erythematosus, psoriasis
alleviated symptoms by cholesterol-lowering medication	systemic lupus erythematosus, psoriasis
improvement of diseases by low-fat diet	rheumatoid arthritis, systemic lupus erythematosus, psoriasis
exacerbation of diseases by high-fat diet	multiple sclerosis, type I diabetes

circulating triglycerides and cholesterols[17]. Moreover, cholesterol-lowering treatment such as statins and low-fat diet has been shown to ameliorate psoriasis and SLE, suggesting a detrimental role of hyperlipidemia in the autoimmune diseases[13, 14]. Although much is known about the tight association of atherosclerosis and autoimmune diseases, the mechanism by which atherogenic dyslipidemia modulates autoimmune T cell and B cell responses remains elusive.

4. Lipid-activated transcription factors

Lipid metabolism is a process of dynamic flux of multiple lipid species that are essential for energy homeostasis, cellular structure and signaling. This process is regulated by nuclear receptors. Nuclear receptors are transcription factors that are activated by ligand, linking lipid signaling to the expression of target genes. For example, oxysterols activate liver X receptor (LXR), fatty acid and fatty acid metabolites regulate peroxisome proliferator- associated receptor γ (PPARγ), and retinoic acids are recognized by retinoid X receptor (RXR) and retinoic acid receptor (RAR) (**Figure 5**). These nuclear receptors form heterodimers or homodimer with RXR, and categorized into permissive and non-permissive groups (**Figure 6**). Heterodimer containing LXR and PPAR with RXR can be activated by either agonist and called permissive. While non-permissive RAR/RXR heterodimer only can be activated by RAR ligands[18].

Among lipid-activated transcription factors, LXR has two isoforms referred as LXRα (encoded by *Nr1h3*) and LXRβ (encoded by *Nr1h2*). Although they share similar structure and function, LXRα is mostly expressed by metabolically active tissues, such as liver, while LXRβ is universally expressed by all types of cells. LXR activation prevents cholesterol accumulation in cells by upregulating its target *Abca1* and *Abcag1*, which increases cholesterol efflux[19].

Emerging evidence shows that lipid metabolism and immune function are inter-regulated. It is well-documented that alteration in lipid homeostasis, such as the pathogenesis of obesity and cardiovascular diseases, is associated with chronic inflammation, which leads inflammatory polarization of macrophages and T cells. Activation of lipid-activated transcription factors are, but still controversial, believed to serve as immunoregulatory roles[18, 19, 20, 21]. LXR and PPARγ agonist inhibits

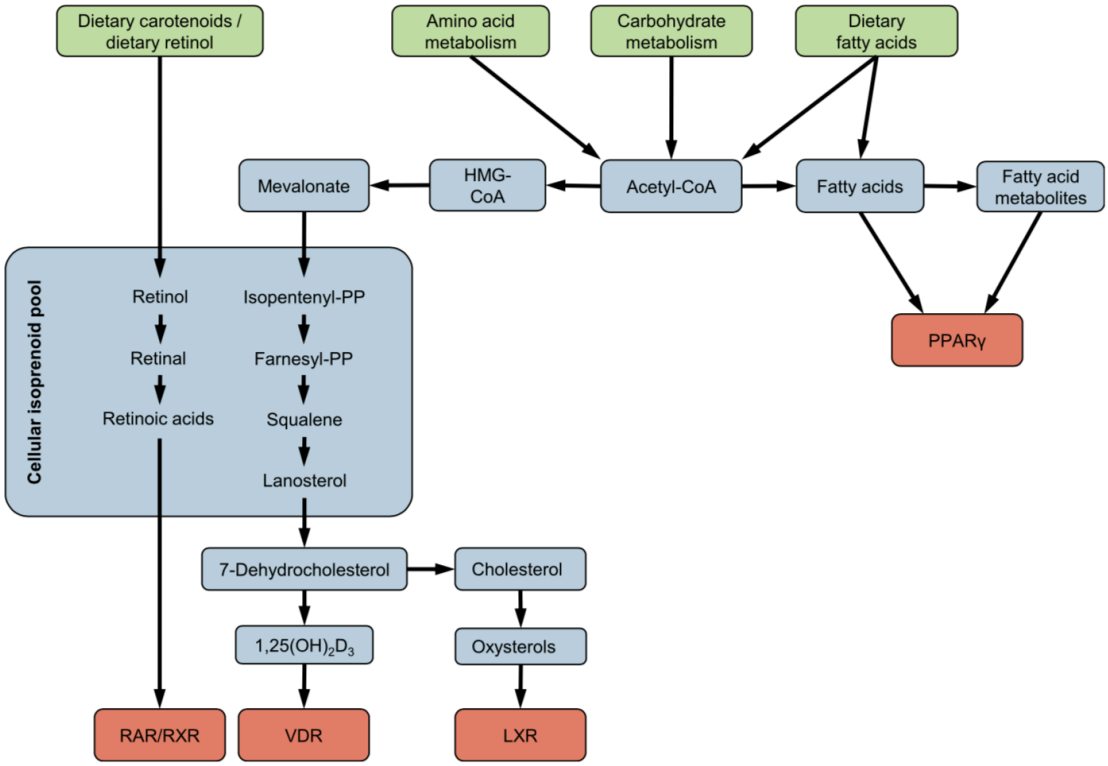

Figure 5. *Pathway of lipid metabolism providing ligands for lipid-activated transcription factors*[17]

Lipid-activated transcription factors are activated by various types of lipid including cellular products of isoprenoid pathway.

proinflammatory molecules such as iNOS, COX-2, IL-6, IL-12, and IL-27[18, 21]. Also, LXR links immune signaling by regulating toll-like receptor 4 (TLR4) expression, mediating LPS recognition[19]. Retinoid receptors promote polarization of macrophage from proinflammatory M1 which secretes TNF-α and IL-12 to anti-inflammatory phenotype, which produce immunoregulatory cytokine IL-10, presumably through suppression of NF-κB[18]. LXR activation in T cell inhibits T_H1 and T_H2 cells while its role in T_H17 and T_{FEG} cells remains controversial[22, 23]. Role of LXR in T_{FH} cells remains to be elucidated. PPARγ deficiency promotes T_H1, T_H17 differentiation while suppressing T_{REG} cells[24]. Taken together, lipid-activated transcription factors may serve as immunoregulatory function in immune cells.

Several drugs targeting lipid-activated transcription factors have been developed and approved by FDA; however, no FDA-approved drug has been developed targeting

LXR (**Table 3**)[18]. Some retinoid receptor and PPARγ agonists have been effective for patients with SLE, RA, and inflammatory bowel diseases (IBD) in human clinical trials (**Table 4**)[18] and LXR agonists also ameliorated SLE phenotypes and decreased autoantibody production in murine model[25]. However, little is known whether and how lipid-activated transcription factors may affect antibody production.

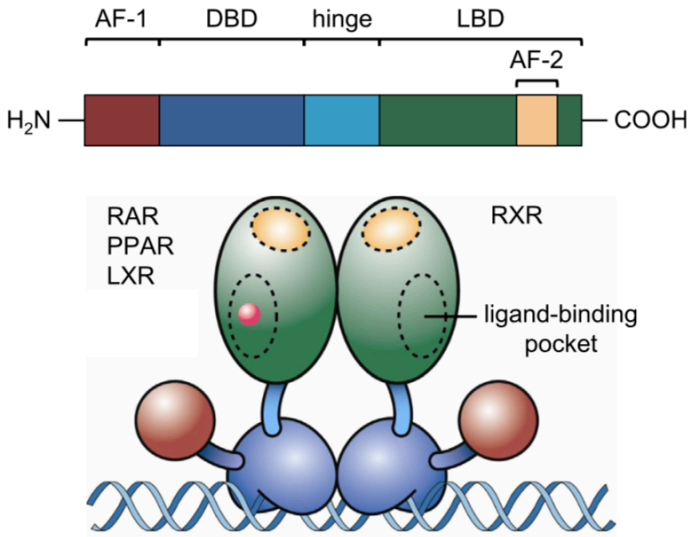

***Figure 6**. Structure of lipid-activated transcription factors*[17]

RXR forms heterodimers with RAR, PPAR, or LXR. AF-1, ligand-independent activation function; AF-2, ligand-dependent activation function; DBD, DNA-binding domain, hinge region.

Table 3. List of FDA-approved drugs targeting lipid-activated transcription factors[17]

Nuclear receptor	Physiological lipid ligand(s)	FDA-approved drugs targeting the receptor (based on Rask-Andersen et al Table S1[365])	
		Drug name	Therapeutic class
RAR	ATRA	Adapalene	Dermatologic agent
		Alitretinoin	Antineoplastic agent
		Isotretinoin	Keratolytic agent
		Acitretin	Keratolytic agent
		Tazarotene	Keratolytic agent
		Tretinoin	Antineoplastic agent, keratolytic agent
RXR	9-cis-RA	Bexarotene	Antineoplastic agent
		Alitretinoin	Antineoplastic agent
		Tazarotene	Keratolytic agent
		Tretinoin	Antineoplastic agent, keratolytic agent
LXR	22(R)-hydroxycholesterol 24(S)-hydroxycholesterol 24(S),25-epoxycholesterol 27-hydroxycholesterol	No FDA-approved ligand available	
PPARγ	Unsaturated fatty acids	Pioglitazone	Hypoglycemic agent
	15d-PGJ	Rosiglitazone	Hypoglycemic agent
	12-HETE, 15-HETE	Treprostinil	Antihypertensive agent; antithrombotic agent
	9-HODE, 13-HODE		
	oxLDL-derivatives		
	LPA		
	Serotonin metabolites		

Table 4. List of human clinical studies targeting lipid-activated transcription factors in patients with RA, IBD, and SLE[17]

RA				IBD			
Authors	**No.**	**Drug(s) used**	**Results**	**Authors**	**No.**	**Drug(s) used**	**Results**
Vitamin A/retinoids							
				Wright et al, 1985[253]	86	Vitamin A vs placebo	→ Disease activity
PPARγ agonists							
Shahin et al, 2011[201]	49	Usual treatment + pioglitazone vs usual treatment + placebo	↓ Disease activity	Lewis et al, 2008[274]	105	Rosiglitazone vs placebo	↑ Clinical response and remission → Endoscopic remission
				Liang 2008[275]	42	Rosiglitazone + 5-ASA vs 5-ASA	↓ Disease activity
Vitamin D							
Salesi and Farajzadegan, 2011[226]	117	Methotrexate + vitamin D vs methotrexate + placebo	→ Disease activity	Miheller et al, 2009[288]	37	$1,25(OH)_2$ vitamin D_3 vs 25(OH) vitamin D_3	↓ Disease activity (only $1,25[OH]_2D_3$)
Gopinath and Danda, 2011[227]	121	DMARD + calcium + vitamin D vs DMARD + calcium	↑ Pain relief	Jørgensen et al, 2010[289]	108	Vitamin D vs placebo	↓ Relapse rate
Racovan et al, 2012[220]	32,435	Calcium + vitamin D vs placebo	→ RA incidence				

SLE			
Authors	**No.**	**Drug(s) used**	**Results**
Juarez-Rojas et al, 2012[314]	30	Pioglitazone vs placebo	↑ HDL cholesterol ↓ Insulin resistance ↓ CRP
Abou-Raya et al, 2012[319]	267	Vitamin D vs placebo	↓ Disease activity

II. Purpose of this study

Systemic lupus erythematosus (SLE) is an antibody-mediated autoimmune disease, which leads significant damage in multiple organs by their own immune system. Despite of increasing prevalence and incidence rate of SLE world-widely, and numerous studies and clinical trials proposed to cure the disease, no clear mechanism by which SLE is processed has been suggested. Meanwhile, the incidence of atherosclerosis is significantly increased in patients with SLE. Despite the evident association between atherosclerosis and autoimmune SLE, little is known whether and how hyperlipidemic condition impacts the pathogenesis of SLE. In this regard, I will examine a new mechanistic insight of pathogenesis of SLE; hyperlipidemic environment or lipid metabolism may impact autoimmunity.

Since atherosclerosis-related autoimmune diseases such as SLE, rheumatoid arthritis, and psoriasis are mediated by autoantibodies, I will focus on antibody-generating mechanism, germinal center reactions. Germinal center reactions occur in secondary lymphoid organs where follicular helper T (T_{FH}) cells, germinal center B cell (GC B), plasma cell (PC) play critical roles.

Lipid-activated transcription factors such as LXR, PPAR, and RXR link lipid signaling to the expression of their target genes. Emerging evidence shows that lipid metabolism and immune function are cross-regulated. For example, during the development of metabolic diseases such as obesity and cardiovascular diseases leads chronic inflammation. Thus, understanding the mutual relationship between lipid metabolism and immune cell is crucial. Activation of lipid-activated transcription factors is known to promote immunoregulatory role of immune cells such as polarization of macrophages and differentiation of T cells. However, the role of lipid-activated transcription factors in antibody production or germinal center reaction is not clearly understood and no effective drugs have been developed specifically targeting LXR for SLE therapy.

In this study, the role of T_{FH} cells in the pathogenesis of atherosclerosis-induced SLE will be proposed by analyzing *Apoe*$^{-/-}$ and *Ldlr*$^{-/-}$ recipients of lupus-prone BXD2 bone marrow. Functional changes of T_{FH} cells will be analyzed by transcriptome analysis and T_{FH} subset analysis. Also, the mechanism by which the functional changes of T_{FH} cells are proceeded will be discussed by utilizing IL-27EBI3-, TLR4-, LXR-, and

STATs-deficient mice. Clinical relevance will be implicated by analyzing plasma samples of patients with hypercholesterolemia and healthy individuals.

III. Materials and methods

Ethics statement

All experiments were performed according to protocols approved by the Institutional Animal Care and Use Committees of Seoul National University (SNU-160422-3-3). Applicable human subject protocols were approved by the Institutional Review Boards at Seoul National University (E1707/001-006) and Yonsei University (4-2016-1010). All subjects provided informed consent. The characteristics of each subject are provided in **Table 5**.

Mice

Apoe$^{-/-}$, BXD2, *Ebi3*$^{-/-}$, *Ldlr*$^{-/-}$, and *Il27ra*$^{-/-}$mice were purchased from Jackson Laboratory (Maine, USA). *Tlr4*$^{-/-}$ and *Stat3*$^{f/f}$ were kindly provided by Drs. Seung-Yong Sung and Shuzuo Akira. *Stat1*$^{-/-}$ mice were kindly provided by Dr. Hun Sik Kim (Ulsan University). *Nr1h2*$^{-/-}$ mice were kindly provided by Won-il Jeong (Korea Advanced Institute of Science and Technology). C57BL/6 mice were purchased from Orient Bio (Gyeonggi, South Korea). List of mouse strains and primer sequences for genotyping are provided in **Table 6**. Female mice were used throughout all experiments. *Ebi3*$^{-/-}$*Apoe*$^{-/-}$ mice were generated by the interbreeding of *Ebi3*$^{-/-}$ and *Apoe*$^{-/-}$mice. In some experiments, we established bone marrow (BM) chimeric mice. In brief, 7-8-week-old mice were injected with busulfan in DMSO (50 mg/kg, i.p.) to ablate BM in the recipient mice, and BM cells from the indicated mice were adoptively transferred. The recipients were maintained on normal chow diet for 6 weeks of reconstitution period before additional treatment. All mice were bred and maintained under specific pathogen-free facility at the vivarium of the Seoul National University, with free access to gamma-irradiated standard cereal-based diets (Ziegler) or gamma-irradiated high fat diets (40 % energy from fat) (Research Diets, New Brunswick, USA).

Table 5. Clinical characteristics of cohorts

	controls	**patients**
total n	24	24
male (%)	37.5	37.5
age (years)	51.42±2.57	52.25±2.89
body mass index (kg/m^2)	24.25±0.52	25.43±1.02
lipid profile (mg/dl)		
total cholesterol	185.3±9.33	328.6±9.70***
LDL cholesterol	99.31±3.81	262.5±6.62***
HDL cholesterol	48.95±4.73	44.33±1.86
triglycerides	163.8±31.05	168.5±16.27
comorbidity (%)		
diabetes mellitus	4.17	12
hypertension	37.5	58.3
current smoking	16.7	12.5
coronary artery disease	8.33	58.3
drugs (%)		
beta blocker	0	33.3
ACEI/ ARB	12.5	50
CCB	4.17	33.3
diuretics	0	12.5
anti platelet	0	50
anti diabetes	0	12.5

Table 6. List of mice strains used in this study and genotyping sequences of the mice

Strain	Forward	Reverse
Apoe$^{-/-}$	GCC TAG CCG AGG GAG AGC CG (common)	TGT GAC TTG GGA GCT CTG CAG C (WT)
		GCC GCC CCG ACT GCA TCT (Mut)
BXD2	Not applicable	
Ebi3$^{-/-}$	AAC CTC AGG CCA GGC AGT	TTC CGT AGG CCA TGT AGG AC (WT)
	–	GCC AGA GGC CAC TTG TGT AG (Mut)
Ldlr$^{-/-}$	TAT GCA TCC CCA GTC TTT GG	CTA CCC AAC CAG CCC CTT AC (WT)
	–	ATA GAT TCG CCC TTG TGT CC (Mut)
Il27ra$^{-/-}$	CAA GAC CTT GTG TGC AGG TG (WT)	GTC ACC ATC TTG AGC CCA GT (WT)
	CTT GGG TGG AGA GGC TAT TC (Mut)	AGG TGA GAT GAC AGG AGA TC (Mut)
Tlr4$^{-/-}$	CTA ATG GAT TTG CTG CCT GAC (common)	TCC TGG GGA AAA ACT CTG G (WT)
		CCT GGA AAG GAA GGT GTC AG (Mut)
Stat3$^{f/f}$	CCT GAA GAC CAA GTT CAT CTG TGT GAC	CAC ACA AGC CAT CAA ACT CTG GTC TCC
Stat1$^{-/-}$	CTA CCA GAG TAT CTG CCT AGA C (WT)	CCT CTC AAC CTT CCT GAC ACC (WT)
	CTG TGC TCG ACG TTG TCA CTG (Mut)	CTC TTC GTC CAG ATC ATC CTG (Mut)
Nr1h2$^{-/-}$	CTG TCT TTT GGT CCG CTT TC (common)	CAC CCC TTG CTT ACA CTG CT (WT)
	–	CCA GTC ATA GCC GAA TAG CC (Mut)

Immunization

WT, *Apoe*$^{-/-}$, *Ebi3*$^{-/-}$*Apoe*$^{-/-}$or the recipient mice in the bone marrow chimerism studies were subcutaneously immunized with 100 μg of Keyhole limpet hemocyanin (KLH) (Sigma) or NP-OVA (Biosearch Technologies) emulsified in CFA. Seven days later, lymphoid cells from the spleens and the draining lymph nodes were analyzed.

Immunohistochemical Analysis

Spleens or kidneys from mice were embedded in Tissue-Tek O.C.T compound (Sakura Finetek, Torrance, CA), and cut into 7 μm sections. The slides were incubated with 3 % BSA/PBS for 30 min, and then stained with FITC Peanut Agglutinin (PNA, Sigma), PE anti-IgD (11-26c.2a, Biolegend), FITC anti-C3 (MP), or FITC anti-IgG (Sigma). The slides were mounted with ProLong® Gold Antifade Reagent (Molecular Probes). Kidneys were incubated in 4 % formalin for 12 h at 4 °C for fixation, and were sent to the Pathology Center at Seoul National University College of Medicine for hematoxylin and eosin staining. Images were acquired with Vectra 3.0 Automated Quantitative Pathology Imaging System (PerkinElmer) and analyzed with inForm (PerkinElmer).

Flow cytometry

Lymphoid cells were obtained and stained with PerCp-Cy5.5 or APC-Cy7 anti-CD4 (GK1.5, ThermoFisher), FITC anti-PD-1 (J43, ThermoFisher), biotin anti-CXCR5 (L138D7, Biolegend), APC streptavidin (Biolegend), PE anti-CXCR3 (CXCR3-173, ThermoFisher), PE-Cy7 anti-CCR6 (29-2L17, Biolegend), FITC anti-GL-7 (GL7, Biolegend), PE anti-CD95 (15A7, ThermoFisher), PerCp-Cy5.5 anti-CD138 (281-2, Biolegend), Alexa488 anti-CD62L (MEL-14, Biolegend), PE-Cy7 anti-CD44 (IM7, Biolegend), PE anti-CD25 (PC61, Biolegend), PE anti-IgD (11-26c.2a, Biolegend), APC anti-B220 (RA3-6B2, Biolegend), APC anti-F4/80 (BM8, Biolegend), APC-Cy7 anti-I-A/I-E (M5/114.15.2, Biolegend), PerCp-Cy5.5 anti-CD11c (N418, Biolegend), FITC anti-CD11b (M1/70, Biolegend), or PE-Cy7 anti-CD8a (53-6.7, Biolegend). Transcription factor stainings were performed by using Foxp3/Transcription factor staining buffer set (ThermoFisher) and eFluor450 anti-FOXP3 (FJK-16S, ThermoFisher). For BODIPY staining, lymphoid cells were incubated with 1 μM BODIPY in dark for 30

minutes before washing. For STAT staining, cells were permeabilized with methanol for 30 minutes after fixation, and were stained with Alexa647 anti-STAT1 (4a, BD Bioscience) or Pacific Blue anti-STAT3 (4/P-STAT3, BD Bioscience). The cells were analyzed with FACS Verse, LSRFortessa, AriaIII or Calibur (BD Bioscience, San Jose, CA), and data were analyzed using FlowJo software (TreeStar, Ashland, OR).

Cell isolation and differentiation

For preparation of primary DCs, spleens were surgically removed and teased into small pieces by using gentleMACS^{TM} dissociator (Miltenyi Biotec, Bergisch Gladbach, Germany), and digested with RPMI 1640 medium containing 10% of FBS, 0.5 mg/ml of collagenase (ThermoFisher) and 30 μg/ml of DNase I (Bio Basic Inco.) for 30 min at 37 °C. Then, $CD11c^+$ cells were isolated by MACS (Miltenyi Biotec). Isolated DCs were stimulated with LPS (100 ng/ml, Sigma) for four hours (for RT-PCR) or 24 hours (for ELISA). $CD4^+$ T cells were isolated by MACS (Miltenyi Biotec) and the cells were further sorted as T_{FH} cells ($CD4^+PD\text{-}1^+CXCR5^+$) by FACSAria III flow cytometer (BD Bioscience). Naive B cells ($B220^+GL\text{-}7^-IgD^+$, $1x10^5$/well) were isolated by FACSAria III, and, for some experiments, were co-cultured with T_{FH} cells ($4x10^4$/well) for seven days in in RPMI-1640 supplemented with 10 % FBS in presence of anti-CD3 (145.2C11), anti-IFN-γ (XMG1.2) and anti-IgM (AffiniPure $F(ab')_2$ Fragment Goat anti-IgM, μ chain specific, Jackson ImmunoResearch) or LPS plus IL-4 (Peprotech).

ELISA

To measure the levels of antibodies to dsDNA, rheumatoid factors and histone in circulation, sera were collected from mice and were measured by ELISA as described previously[26]. Briefly, ELISA plates (Greiner Bio-one, Germany) were coated with 0.01 % of poly-L-lysine (Sigma-Aldrich) for 1 hour prior to coating with 5 μg/ml of calf thymus dsDNA (Sigma-Aldrich), rabbit IgG (Sigma-Aldrich) and 5 μ g/ml of histone (from calf thymus, Sigma-Aldrich) overnight at 4°C. The plates were blocked for 2 hours with 5 % skim milk in PBS. Sera were diluted in the same solution, were transferred to the plates and were incubated for 2 hours at room temperature. Then the assay was performed with HRP-conjugated total IgG, IgG1, IgG2b, or IgG2c (all from SouthernBiotech) detection

antibody. To measure the levels of IgG in culture supernatants or sera, IgG were quantified with a total IgG capture antibody (Donkey anti-mouse IgG (H+L), Jackson ImmunoResearch, West Grove, PA) and HRP-conjugated IgG, IgG1, IgG2b, or IgG2c detection antibody. Sera from OVA-NP immunized mice were collected, and NP-specific IgG, IgG1, IgG2b and IgG2c antibodies were measured by NP-BSA (Biosearch Technologies) ELISA. Other ELISA kits, including IL-27, human IgG, IgG1, IgG3, and IgG4 were purchased from ThermoFisher, and were conducted as described in manufacturer's instruction.

RT-PCR

Total RNA was prepared by using Trizol (Invitrogen), and cDNA were synthesized with RevertAid First Strand cDNA Synthesis Kit (ThermoFisher) according to the manufacturer's protocol. Gene expression was measured by quantitative 7500 Fast RT-PCR (Applied Biosystems). The levels of gene expression were normalized to *Actb*. The primer pairs used in quantitative RT-PCR are described in **Table 7**.

Western blot

$CD11c^+$ dendritic cells were isolated from the indicated mice by MACS (Miltenyi Biotec). Naïve B cells ($B220^+CD138^-GL7^-CD95^-IgD^+$), germinal center B cells ($B220^+CD138^-GL7^+CD95^+$), plasma cell ($B220^{-/int}CD138^+$), memory B cells ($B220^+CD138^-GL7^-CD95^-IgD^-CD27^+$) were sorted by FACSAria III flow cytometer (BD Bioscience). Cells were washed with cold PBS, lysed with RIPA lysis buffer containing protease inhibitor cocktail (GenDepot) and cell lysates (40 μg of proteins) were used for SDS-PAGE, transferred to Immobilon-P PVDF membrane (Millipore). The blots were blocked with 5 % nonfat dry milk in TBST (0.05 %), and probed with antibodies at 4 °C overnight. The following antibodies were used for Western blot analysis: anti-LXRβ (14278-1-AP, 1:2000 dilution, Proteintech), anti-β-actin (sc-47778, 1:1000 dilution, Santa Cruz Biotechnology), anti-

Table 7. List of RT-PCR primer sequences

Gene	Sequence	
	Sense (5'->3')	anti-sense(5'->3')
Ifng	GATGCATTCATGAGTATTGCCAAGT	GTGGACCACTCGGATGAGCTC
Hist1h3g	CTACCTCGTGGGTCTGTTTG	CAGAAACCCTTAAGCCCTCT
S100a8	TGGTCACTACTGAGTGTCCT	CTACTCCTTGTGGCTGTCTT
Ifitm1	CCTGTCCCTAGACTTCACGG	GACCATGTGATCTGGTCCCT
Ifitm2	CCACCATCTTCCTGTCCCTA	TGGTCTGGTCCCTGTTCAAT
Bcl6	CACACCCGTCCATCATTGAA	TGTCCTCACGGTGCCTTTTT
Cxcr5	ACTCCTTACCACAGTGCACCT	GGAAACGGGAGGTGAACCA
Il21	TCATCATTGACCTCGTGGCCC	ATCGTACTTCTCCACTTGCAATCCC
Il4	AGATCACGGCATTTTGAACG	TTTGGCACATCCATCTCCG
Slamf5	ATGGCCCAGCGCCATCTGTGGATC	TCTTGGTGATGGTTTCCTCA
Cxcr3	CAGCCTGAACTTTGACAGAACCT	GCAGCCCCAGCAAGAAGA
Ebi3	TCCCCGAGGTGCACCTGTTCTCC	GGTCCTGAGCTGACACCTGG
Il12a	CCACCCTTGCCCTCCTAAAC	GGCAGCTCCCTCTTGTTGTG
Il12b	CTTGCAGATGAAGCCTTTGAAGA	GGAACGCACCTTTCTGGTTACA
Il27	CTCTGCTTCCTCGCTACCAC	GGGGCAGCTTCTTTTCTTCT
Il23a	AAGTTCTCTCCTCTTCCCTGTCGC	TCTTGTGGAGCAGCAGATGTGAG
Il6	CTCTGGGA AATCGTGGAAATG	AAGTGCATCATCGTTGTTCATACA
Tlr2	TTGCTCCTGCGAACTCCT	AGCCTGGTGACATTCCAA
Tlr4	TCCGGAAGTTCACATAGC	TCCATCTCACAAGGCATG
Olr1	CAAGATGAAGCCTGCGAATGA	ACCTGGCGTAATTGTGTCCAC
Cd36	GCATGGCAGCTTTGGGCAGG	TGCACAGGAGAGGCGGGCAT
Actin	TGGAATCCTGTGGCATCCATGAAAC	TAAAACGCAGCTCAGTAACAGTCCG
Nr1h3	CCGACAGAGCTTCGTCC	CCCACAGACACTGCACAG
Nr1h2	TACATCGTGGTCATCTTAGAG	GGCACAGCTCATGGC
Srebf1	GCCATGGATTGCACATTTGA	GCTGGAGCATGTCTTCGATGT

rabbit IgG-HRP (sc-2004, 1:5000 dilution, Santa Cruz Biotechnology), and anti-mouse IgG-HRP (sc-2005, 1:5000 dilution, Santa Cruz Biotechnology).

Statistics

Data were analyzed with GraphPad Prism 7 (GraphPad Software, La Jolla, CA, USA). Statistics were calculated with the two-tailed Student's *t*-test. *p*-values are presented within each figure or figure legend.

Data availability

The data that support the findings of this study are available from the corresponding author upon request. RNA-seq data have been deposited in the Gene Expression Omnibus under accession code GSE111779.

IV. Results

1. Exacerbation of lupus-like symptoms in hyperlipidemic condition

As a first step to investigate the role of atherogenic dyslipidemia in autoimmune lupus, the levels of autoantibodies and severity of lupus phenotypes were examined under atherogenic environment *in vivo*. To develop lupus-like phenotype under atherogenic condition, bone marrow cells from lupus-prone BXD2 mice[26] were transferred into bone marrow-ablated wild-type (WT) or Apolipoprotein E (ApoE)-deficient mice (herein referred as to WT^{BXD2} and $ApoE^{BXD2}$, respectively). After six-week of reconstitution period, the recipients were subjected on high-fat diet (HFD) for another six weeks to develop hyperlipidemic condition in $ApoE^{BXD2}$ mice (**Figure 7A**). Histological assessments of kidney indicated that HFD-treated $ApoE^{BXD2}$ mice exhibited more severe glomerulonephritis with expanded Bowman's space, crescentic glomerulus and deposition of IgG immune complex in comparison with HFD-treated WT^{BXD2} mice (**Figure 7B, C**).

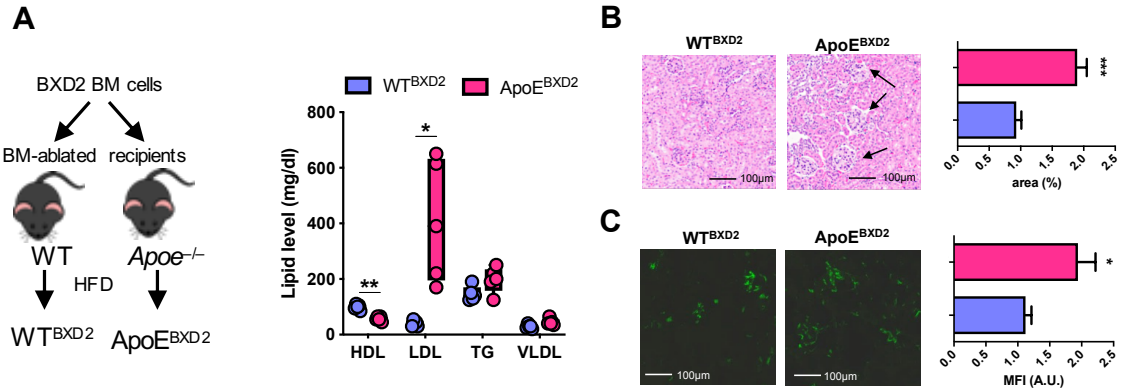

***Figure** 7.Exacerbation of autoimmune glomerulonephritis in Apoe$^{-/-}$ recipients of BXD2 bone marrow*

(A) Experimental procedure (left): WT mice and *Apoe*$^{-/-}$ mice in which the bone marrow was ablated were given intravenous transfer of bone marrow cells from lupus-prone BXD2 mice and were fed an HFD. Right, concentration of high-density lipoprotein (HDL), LDL, triglycerides (TG) and very low-density lipoprotein (VLDL) in plasma from mice.

(B) H&E staining of the kidneys of the mice (left), and quantification of glomerulus area (right) in the kidneys of mice.

(C) Immunofluorescence staining (left) for IgG in the kidneys of the mice, and mean fluorescent intensity (MFI) of IgG (right) in the kidneys of mice.

Data are from one experiment representative of at least three independent experiments.

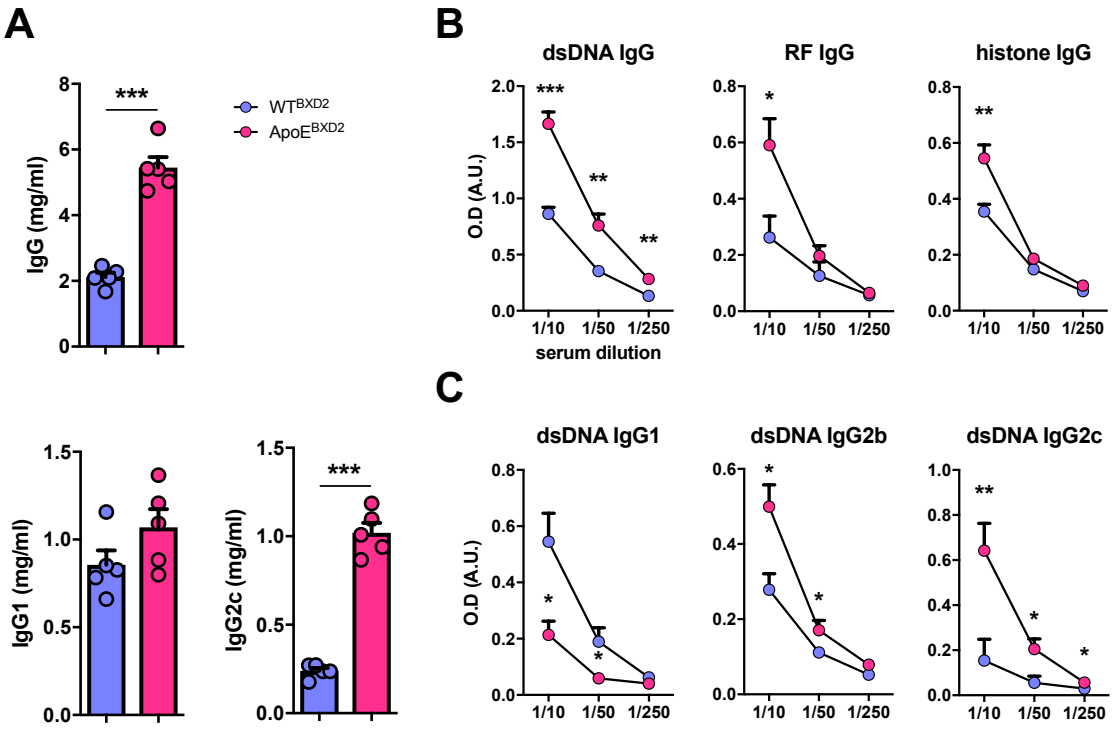

Figure 8. *Augmented autoantibody production in Apoe$^{-/-}$ recipients of BXD2 bone marrow*

(A) ELISA of total IgG, IgG1 and IgG2c antibodies in the serum of the mice as in described in **Figure 7A**.

(B) ELISA of autoantibodies to dsDNA and rheumatoid factor (RF) in the serum of the mice, presented (in arbitrary units (AU)) as optical density (O.D.) measured at 450 nm.

(C) ELISA of autoreactive IgG-subclass autoantibodies to dsDNA in the serum of the mice.

Data are from one experiment representative of at least three independent experiments.

The levels of total IgG and IgG2c, but not IgG1, were significantly higher in the sera of ApoE^{BXD2} than WT^{BXD2} (**Figure 8A**). More importantly, the levels of IgG autoantibodies against dsDNA, rheumatoid factor IgG, and histone IgG, particularly IgG2c isotype, were significantly higher in the former group than the latter (**Figure 8B, C**). IgG2c autoantibodies are known to be more pathogenic than IgG1 in systemic lupus erythematosus (SLE) due to their capacity to activate complement pathway and FcγRs[27]. When the mice maintained on normal chow diet, the levels of autoantibodies were comparable between WT and *Apoe*$^{-/-}$ recipients (**Figure 9**).

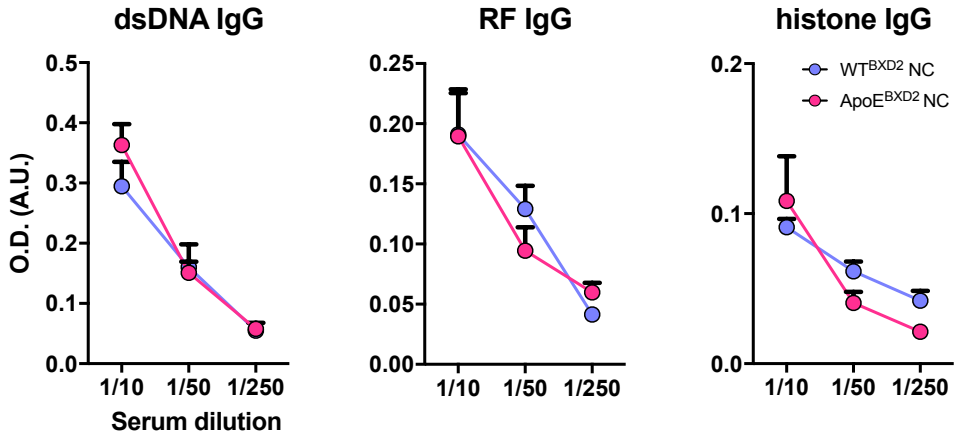

Figure 9. *Comparable autoantibody production in Apoe$^{-/-}$ recipients of BXD2 bone without HFD*

ELISA of autoantibodies to dsDNA and rheumatoid factor (RF) in the serum of the mice described in **Figure 7A** without HFD, presented (in arbitrary units (AU)) as optical density (O.D.) measured at 450 nm.

Data are from one experiment representative of three independent experiments.

Similar experiment with *Ldlr*$^{-/-}$ mice, another widely used animal model of atherosclerosis, exhibited a significantly higher IgG2c autoantibodies and more severe glomerulonephritis than wild-type recipients (**Figure 10A-C & 11A-C**). When lupus-prone BXD2 mice were subjected on HFD, the levels of antibodies and severity of lupus phenotypes were enhanced in HFD group in comparison with those with normal chow diet (**Figure 12A-C**). Taken together, atherogenic dyslipidemia plays a crucial role in augmentation of autoantibody production.

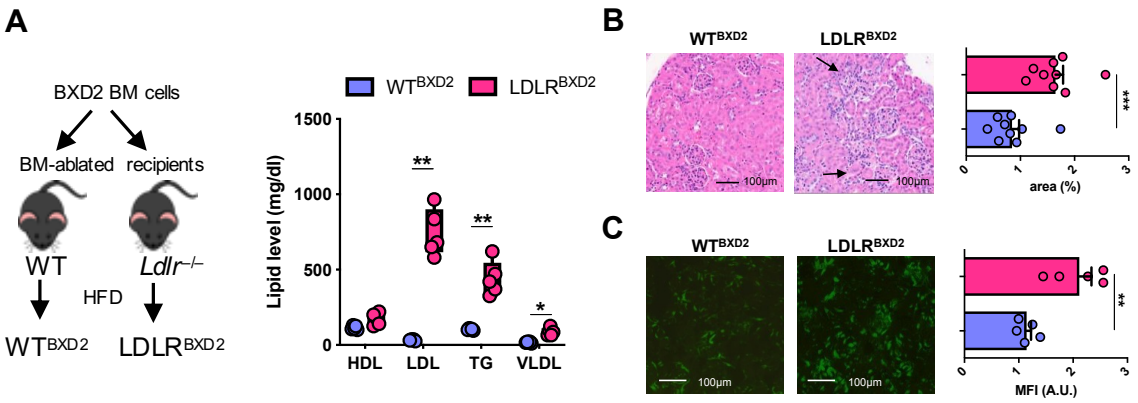

Figure 10. *Exacerbation of autoimmune glomerulonephritis in Ldlr$^{-/-}$ recipients of BXD2 bone marrow*

(A) Experimental procedure (left): WT mice and *Ldlr*$^{-/-}$ mice in which the bone marrow was ablated were given intravenous transfer of bone marrow cells from lupus-prone BXD2 mice and were fed an HFD. Right, concentration of high-density lipoprotein (HDL), LDL, triglycerides (TG) and very low-density lipoprotein (VLDL) in plasma from mice.

(B) H&E staining of the kidneys of the mice (left), and quantification of glomerulus area (right) in the kidneys of mice.

(C) Immunofluorescence staining (left) for IgG in the kidneys of the mice, and mean fluorescent intensity (MFI) of IgG (right) in the kidneys of mice.

Data are from one experiment representative of at least three independent experiments.

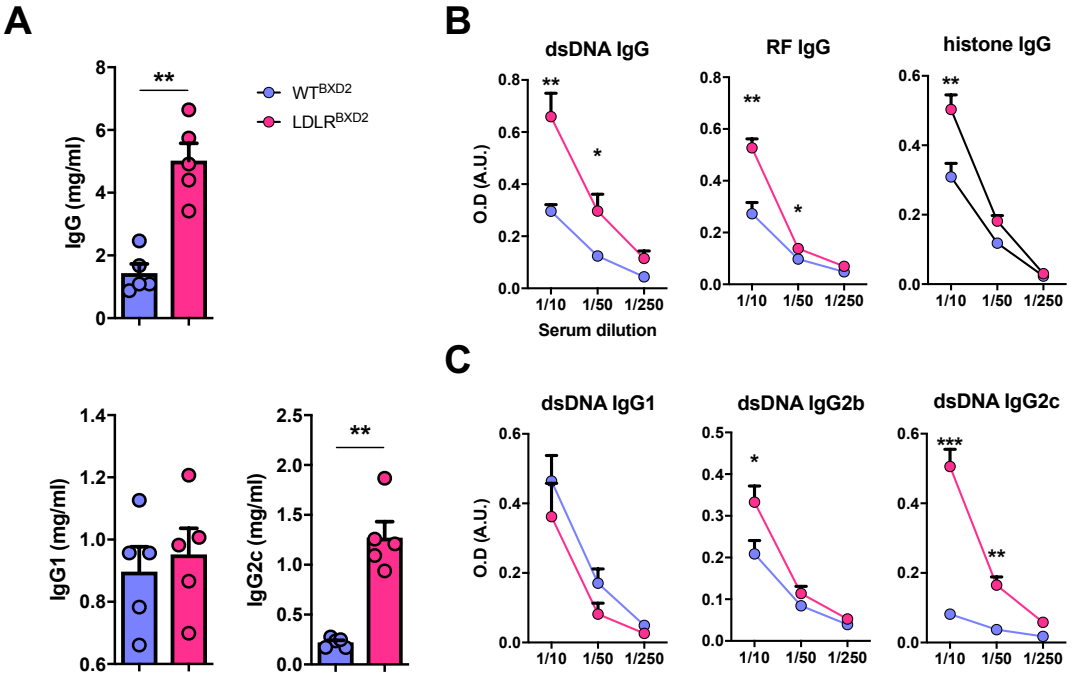

Figure 11. *Augmented autoantibody production in Ldlr$^{-/-}$ recipients of BXD2 bone marrow*

(A) ELISA of total IgG, IgG1 and IgG2c antibodies in the serum of the mice as in described in **Figure 10A**.

(B) ELISA of autoantibodies to dsDNA and rheumatoid factor (RF) in the serum of the mice, presented (in arbitrary units (AU)) as optical density (O.D.) measured at 450 nm.

(C) ELISA of autoreactive IgG-subclass autoantibodies to dsDNA in the serum of the mice.

Data are from one experiment representative of at least three independent experiments.

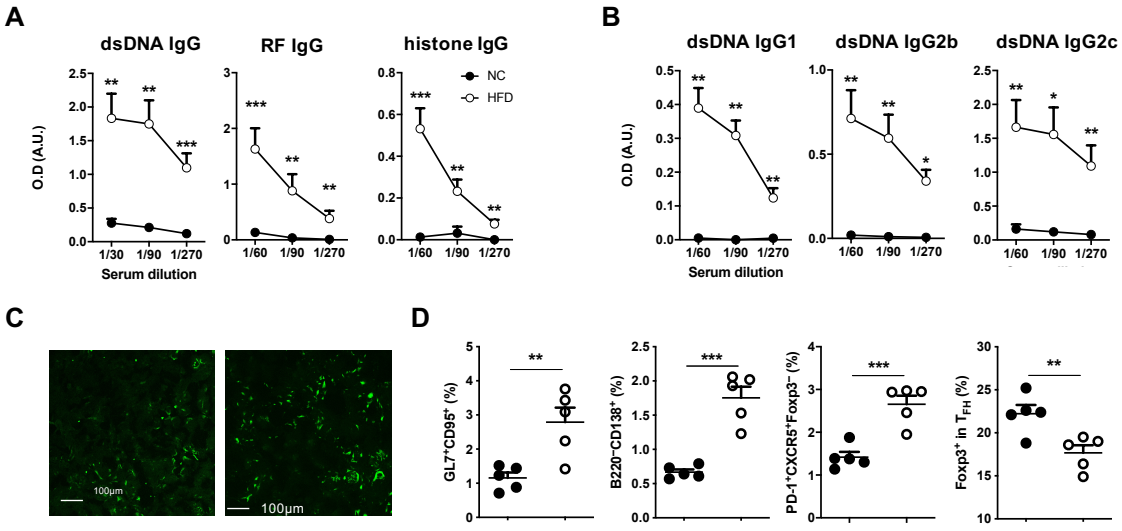

Figure 12. HFD-induced exacerbation of lupus phenotypes in BXD2 mice

(A-D) BXD2 mice were fed a high-fat diet (HFD) for 6 weeks.

(A) ELISA of autoantibodies to dsDNA and rheumatoid factor (RF) in the serum of the mice, presented (in arbitrary units (AU)) as optical density (O.D.) measured at 450 nm.

(B) ELISA of autoreactive IgG-subclass autoantibodies to dsDNA in the serum of the mice.

(C) Immunofluorescence staining for IgG in the kidneys of the mice.

(D) Frequency of $GL7^{+}CD95^{+}$ cells (GC B cells), $B220^{-}CD138^{+}$ cells (plasma cells), PD-$1^{+}CXCR5^{+}Foxp3^{-}$ cells (T_{FH} cells), as well as $Foxp3^{+}$ T_{FH} cells (TFR cells) among splenocytes from the mice, assessed by flow cytometry.

Data are from one experiment representative of three independent experiments.

2. Augmented germinal center reaction under atherogenic environment

Since the levels of autoantibodies were increased, germinal center (GC) reactions, which are responsible for antibody production, spontaneously generated in the recipients of BXD2 bone marrow were assessed. Immunohistochemistry of the spleens revealed that more abundant PNA^+ GCs were found in the spleen in $ApoE^{BXD2}$ mice compared to WT^{BXD2} mice (**Figure 13A**). The frequencies of $GL7^+CD95^+$ GC B cells as well as $B220^-$ $CD138^+$ plasma cells were also higher in $ApoE^{BXD2}$ mice than WT^{BXD2} mice (**Figure 13B, C & Figure 14**). Moreover, the frequency of PD-$1^+CXCR5^+Foxp3^-$ T_{FH} cells, which help B cells to produce antibody, were significantly higher in the $ApoE^{BXD2}$ mice compared to WT^{BXD2} mice (**Figure 13D**), while the frequency of T_{FR} cells were decreased leading increased ratios of T_{FH} or GC B cells to T_{FR} in the $ApoE^{BXD2}$ mice (**Figure 13E,F**). Similarly, lupus-prone BXD2 mice subjected on HFD exhibited higher frequencies of GC B cells, plasma cells, and T_{FH} cells with decrees in T_{FR} cells compared to those with normal chow diet (**Figure 12D**).

To test if the proatherogenic environment also impacts immunization-induced germinal center reactions, HFD-fed WT or *Apoe*$^{-/-}$ mice were immunized with 4-hydroxy-3-nitrophenyl (NP)-conjugated OVA in CFA. The levels of high-affinity and global-affinity NP-specific IgG, particularly IgG2c but not IgG1, were significantly higher in *Apoe*$^{-/-}$ mice than WT mice (**Figure 15A, B**). Consistently, the frequencies of GC B, plasma cells, and T_{FH} cells in the draining lymph nodes were remarkably higher while the frequency of T_{FR} cells were decreased in the former group, leading to increased T_{FH}/T_{FR} and GC-B/T_{FR} ratios (**Figure 16A-E**).

To clarify whether the increased antibody production in atherogenic condition depends on T_{FH} cells, T-B cell interactions were blocked by administration of anti-ICOS antibody to HFD-fed *Apoe*$^{-/-}$ mice immunized with Keyhole limpet hemocyanin (KLH) in CFA. Blockade of T-B cell interaction lead significant decrease in germinal center compartments as well as KLH-specific antibody production (**Figure 17A-C**), suggesting that T_{FH} cells play crucial roles in augmented antibody production under atherogenic condition.

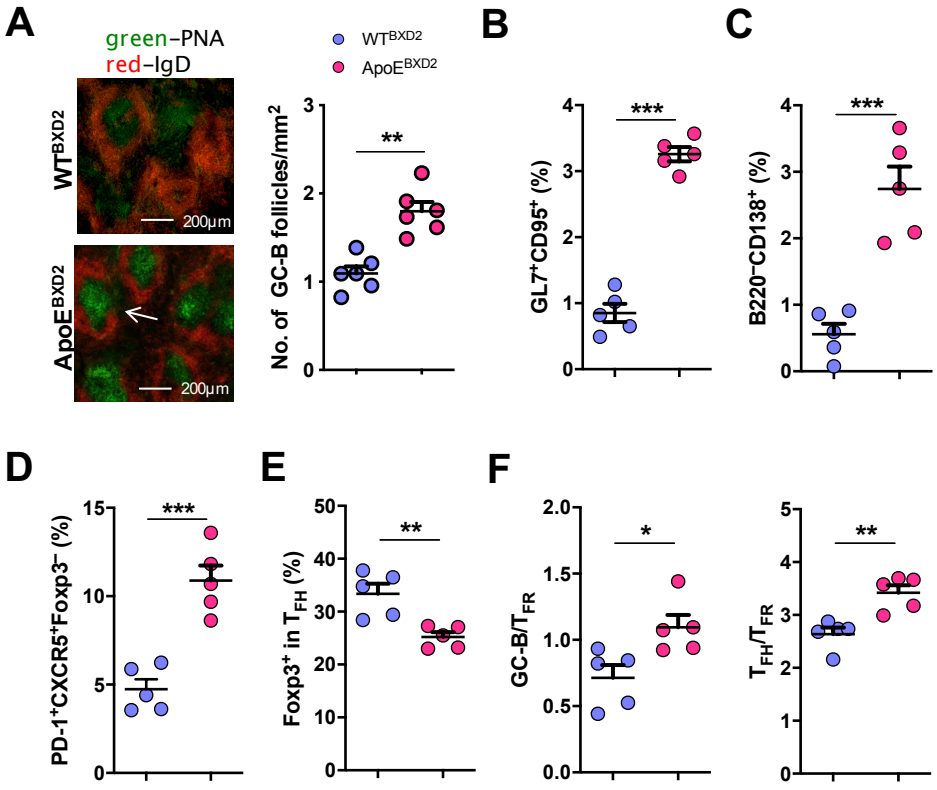

Figure 13. *Enhanced germinal center reactions and T_{FH} cell responses in Apoe$^{-/-}$ recipients of BXD2 bone marrow*

(A) GC staining (left) in the spleen of the mice as described in **Figure 7A**: green, peanut agglutinin; red, IgD. Right, quantification of GC B cell follicles in the spleen of the mice

(B-F) Frequency of $GL7^+CD95^+$ cells (GC B cells)(B), $B220^-CD138^+$ cells (plasma cells)(C), PD- $1^+CXCR5^+Foxp3^-$ cells (T_{FH} cells)(D), and $Foxp3^+$ T_{FH} cells (T_{FR} cells)(E) as well as the ratio of T_{FH} cells to T_{FR} cells (T_{FH}/T_{FR}) and of GC B cells to T_{FR} cells (GC B/T_{FR}) (F), among splenocytes from the mice, assessed by flow cytometry.

Data are from one experiment representative of at least three independent experiments.

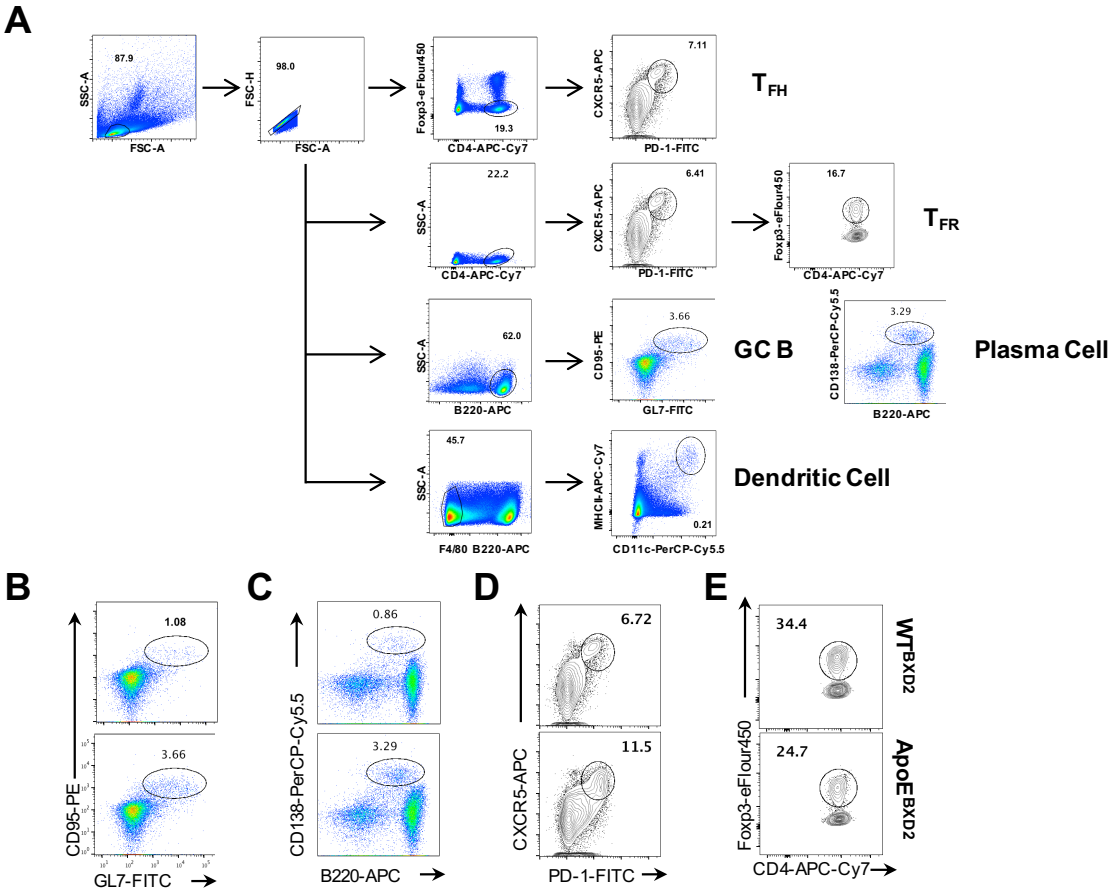

Figure 14. *Analysis strategy for flow cytometry*

(A) Gating strategy used for flow cytometry analysis of each cell types.

(B) Representative flow cytometry data of germinal center B (B), plasma (C), T_{FH} cells (D), and T_{FR} (D) cells in the spleens of the mice as described in **Figure 7A**.

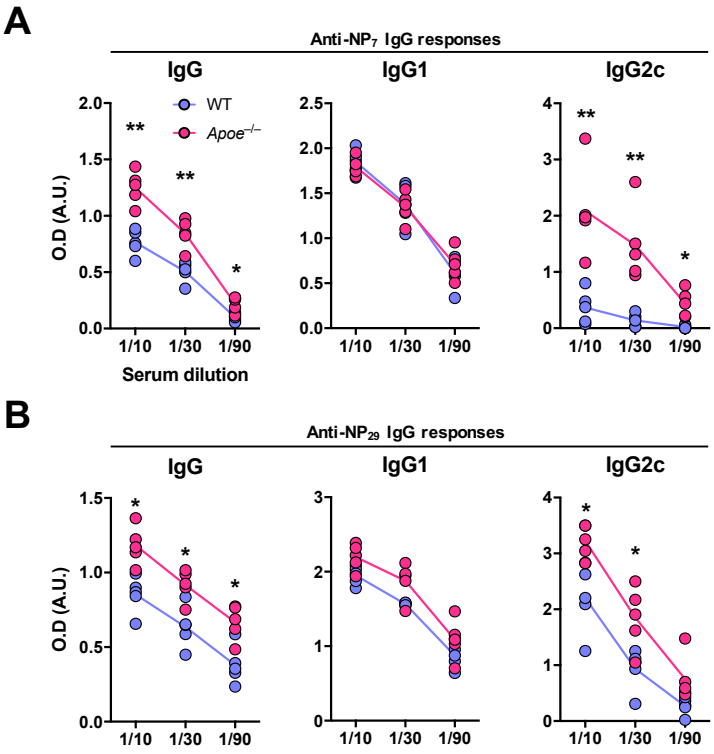

Figure 15. *Elevation of antigen-specific antibody responses in atherogenic mice*

*(*A, B) WT and *Apoe*$^{-/-}$ mice were fed an HFD for 4 weeks before being immunized with OVA-NP in CFA. Mice were analyzed on day 7. ELISA of NP_7-(A) or NP_{29} -(B) specific total IgG, IgG1 and IgG2c antibodies in the serum of the indicated mice.

Data are from one experiment representative of at least three independent experiments.

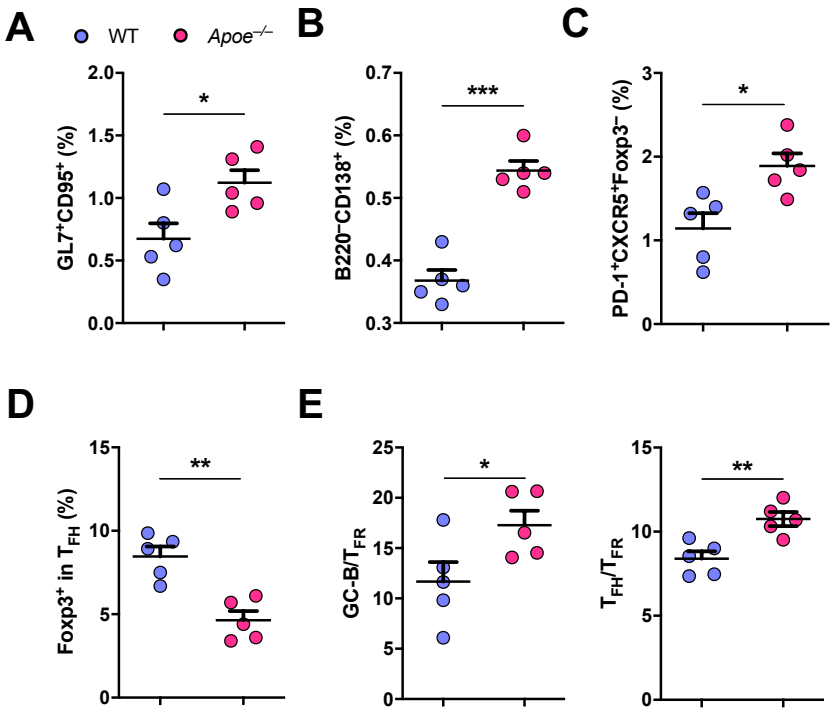

Figure 16. *Augmented germinal center reactions against exogenous antigen in atherogenic mice*

(A-E) Mice were treated and immunized as described in **Figure 15**. Frequency of $GL7^+CD95^+$ cells (GC B cells)(A), $B220^-CD138^+$ cells (plasma cells) (B), PD- $1^+CXCR5^+Foxp3^-$ cells (T_{FH} cells) (C), and $Foxp3^+$ T_{FH} cells (T_{FR} cells) (D) as well as the ratio of T_{FH} cells to T_{FR} cells (T_{FH}/T_{FR}) and of GC B cells to T_{FR} cells (GC B/T_{FR}) (E), among lymphocytes from the mice, assessed by flow cytometry.

Data are from one experiment representative of at least three independent experiments.

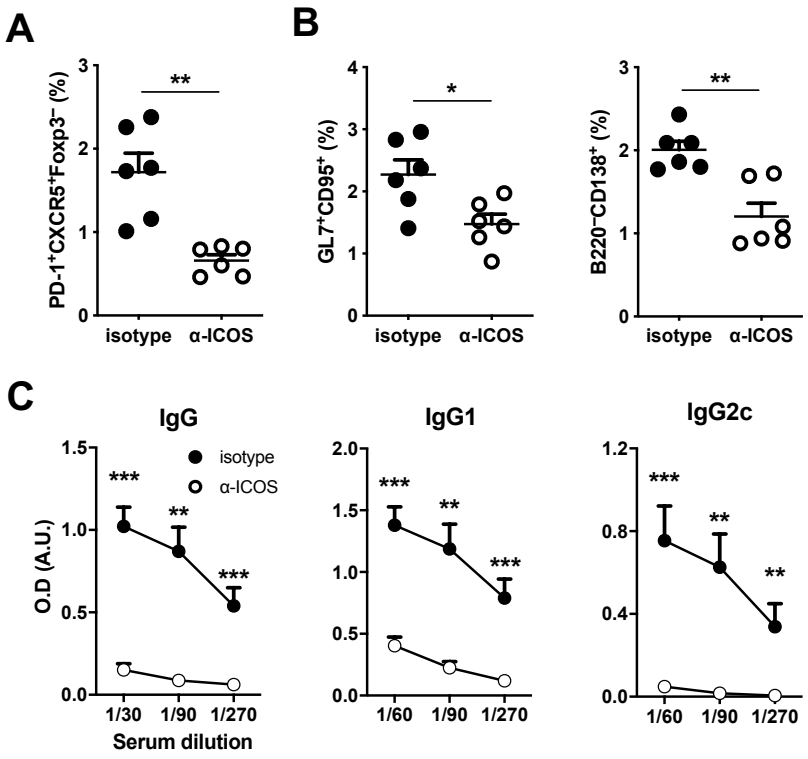

Figure 17. *Essential role of T_{FH} cells in augmented germinal center reaction in atherogenic condition*

(A-C) *Apoe*$^{-/-}$ mice were fed an HFD for 4 weeks, before being injected with KLH in CFA. Each group of mice were injected with control IgG or anti-ICOS antibody intraperitoneally every other day.

(A, B) Frequency of PD- 1^{+}CXCR5^{+}Foxp3^{-} cells (T_{FH} cells) (A), GL7^{+}CD95^{+} cells (GC B cells) (B), and B220^{-}CD138^{+} cells (plasma cells) (C), among lymphocytes from the mice, assessed by flow cytometry.

(C) ELISA of KLH-specific total IgG, IgG1 and IgG2c antibodies in the serum of the indicated mice.

Data are from one experiment representative of two independent experiments.

3. Characterization of T_{FH} cells in hyperlipidemic condition

T_{FH} cells can be subdivided into three subsets based on the surface expression of CXCR3 and CCR6[2]. The frequency and the number of $CXCR3^{+}CCR6^{-}$ T_{FH} population were significantly increased in the $ApoE^{BXD2}$ mice while changes in the $CXCR3^{-}CCR6^{-}$ and $CXCR3^{-}CCR6^{+}$ subpopulations were relatively marginal (**Figure 18A**). Linear regression analyses revealed that the levels of anti-dsDNA IgG exhibited a positive correlation with $CXCR3^{+}CCR6^{-}$ T_{FH} cells (**Figure 18B**). Moreover, the numbers of $CXCR3^{+}CCR6^{-}$ T_{FH} cells were strongly correlated with IgG2c autoantibodies (**Figure 18C)**, suggesting $CXCR3^{+}CCR6^{-}$ T_{FH} cell subset plays important role in triggering the production of IgG2c autoantibodies in this experimental setting.

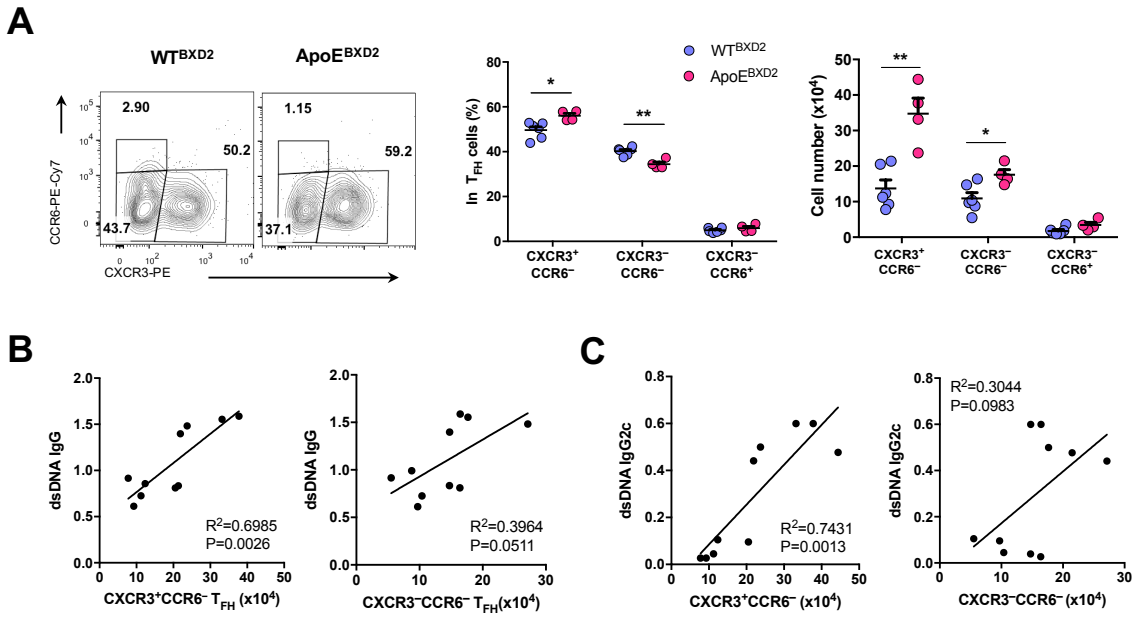

Figure 18. *T_{FH} cell subset analysis of in wild-type or $Apoe^{-/-}$ recipients of BXD2 bone marrow*

(A) Representative flow cytometry data (left half) of T_{FH} cell subset from the spleen of the indicated mice, and frequency (middle) and number (right) of each T_{FH} cell subset (horizontal axis).

(B, C) Linear-regression analysis of the abundance of each T_{FH} cell subset (horizontal axis) and the level of anti-dsDNA IgG (B) or IgG2c (C) in WT^{BXD2} and $ApoE^{BXD2}$ mice.

Data are from one experiment representative of at least three independent experiments.

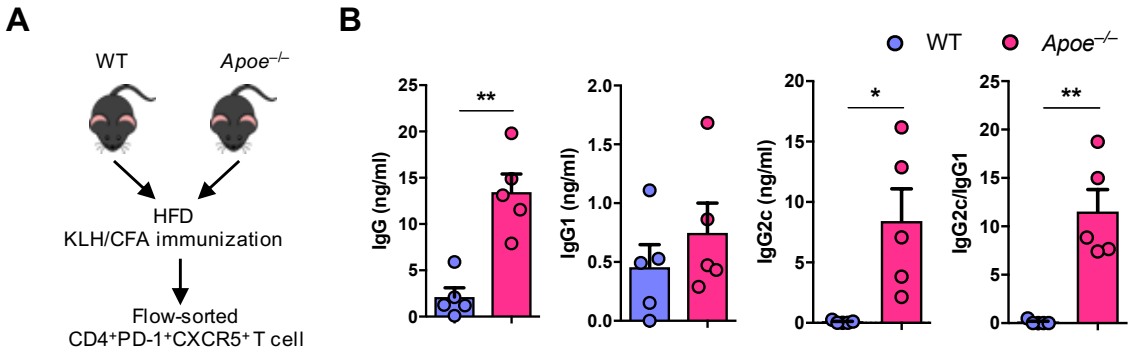

Figure 19. *Profound antibody production by T_{FH} cells generated in atherogenic environment in vitro*

(A) Experimental procedure: WT or *Apoe*$^{-/-}$ mice were immunized with KLH in CFA and fed an HFD, then T_{FH} cells from those mice were sorted by flow cytometry (as $CD4^+PD\text{-}1^+CXCR5^+$) and analyzed further.

(B) ELISA of total IgG, IgG1 and IgG2c, as well as the ratio of IgG2c to IgG1 (IgG2c/IgG1), in supernatants of T_{FH} cells from the mice and naive B cells co-cultured for 7 days in the presence of anti-CD3 and anti-IgM.

Data are from one experiment representative of three independent experiments.

To determine if proatherogenic conditions also impact the B-cell stimulatory function of T_{FH} cells, FACS-sorted T_{FH} cells from HFD-treated WT or *Apoe*$^{-/-}$ mice after immunization with KLH in CFA (**Figure 19A**), and co-cultured them with naive B cells in the presence of anti-CD3 and anti-IgM. T_{FH} cells from *Apoe*$^{-/-}$ mice were far more potent in inducing IgG production from naive B cells than those from WT mice, indicating a qualitative change in T_{FH} cells in the former group in addition to the observed quantitative increase in T_{FH} cell population (**Figure 19B**). IgG subclass analysis revealed that the observed difference in the amount of IgG was mainly due to the increase in IgG2c, but not IgG1. Among T_{FH} subsets obtained from HFD-treated *Apoe*$^{-/-}$ mice, $CXCR3^+$ T_{FH} cells were more potent in inducing IgG2c production from naïve B cells than $CXCR3^-$ T_{FH} cells (**Figure 20A**), which was significantly attenuated by antibody to interferon-γ (IFN-γ) (**Figure 20B**). The number of T_H1 cells and T_H17 cells was also greater in $ApoE^{BXD2}$ mice than in WT^{BXD2} mice (**Figure 20C**); however, $CD44^+CD4^+$ non-T_{FH} cells failed to induce IgG2c production from B cells (**Figure 20D**), suggesting

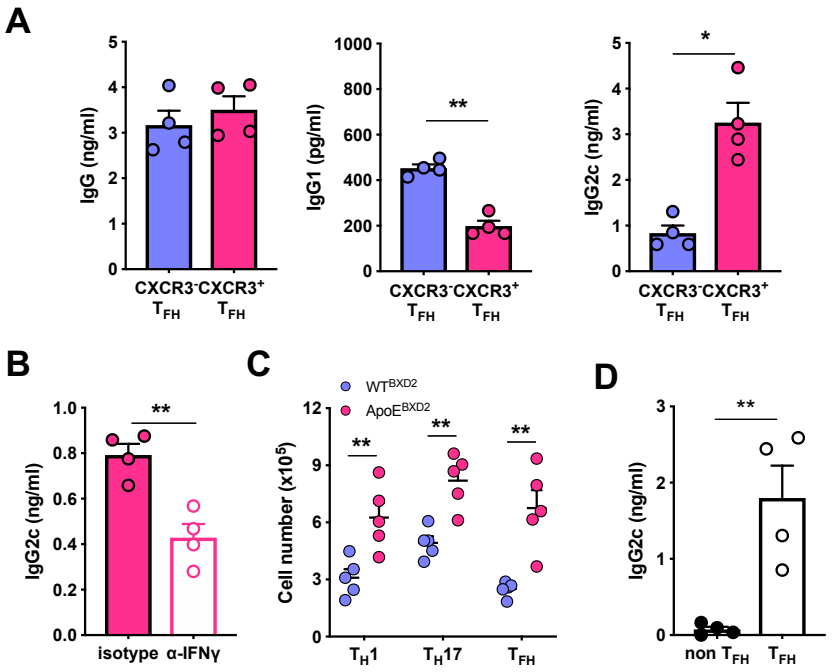

Figure 20. *Regulation of IgG2c production by CXCR3⁺ T_{FH} cells*

(A, B) CXCR3⁺ and CXCR3⁻ T_{FH} cells were flow-sorted from KLH-immunized WT mice. T_{FH} cells and naïve B cells were co-cultured for 7 days in the presence of anti-CD3 and anti-IgM.

(A) ELISA of total IgG, IgG1 and IgG2c in supernatants of the co-culture.

(B) ELISA of IgG2c in supernatants of the co-culture in the absence or presence of anti-IFN-γ.

(C) The number of each T_H cell subset in the indicated mice.

(D) ELISA of IgG2c in supernatants of non-T_{FH} or T_{FH} cells and naive B cells co-cultured.

Data are from one experiment representative of at least three independent experiments.

that rather than non-T_{FH} cells (such as T_H1 cells), T_{FH} cells were responsible for the greater production of IgG2c in the atherogenic mice.

To further characterize the pathogenic features of T_{FH} cells generated in atherogenic conditions, transcriptome analysis of these cells was performed by RNA sequencing (RNA-seq) on the T_{FH} cells isolated from the lymph nodes of HFD-fed WT and *Apoe*$^{-/-}$ mice. At a setting of greater than two-fold expression changes, p value < 0.05, and false discovery rate (FDR) < 0.1, 211 genes were upregulated and 142 genes were downregulated in the T_{FH} cells from *Apoe*$^{-/-}$ mice compared with those from WT mice

(**Figure 21A**). Gene ontology terms analysis of these genes revealed a significant enrichment of inflammatory response, systemic lupus erythematosus, and interferon-γ-related pathway in the T_{FH} cells from the atherogenic mice, which were confirmed by

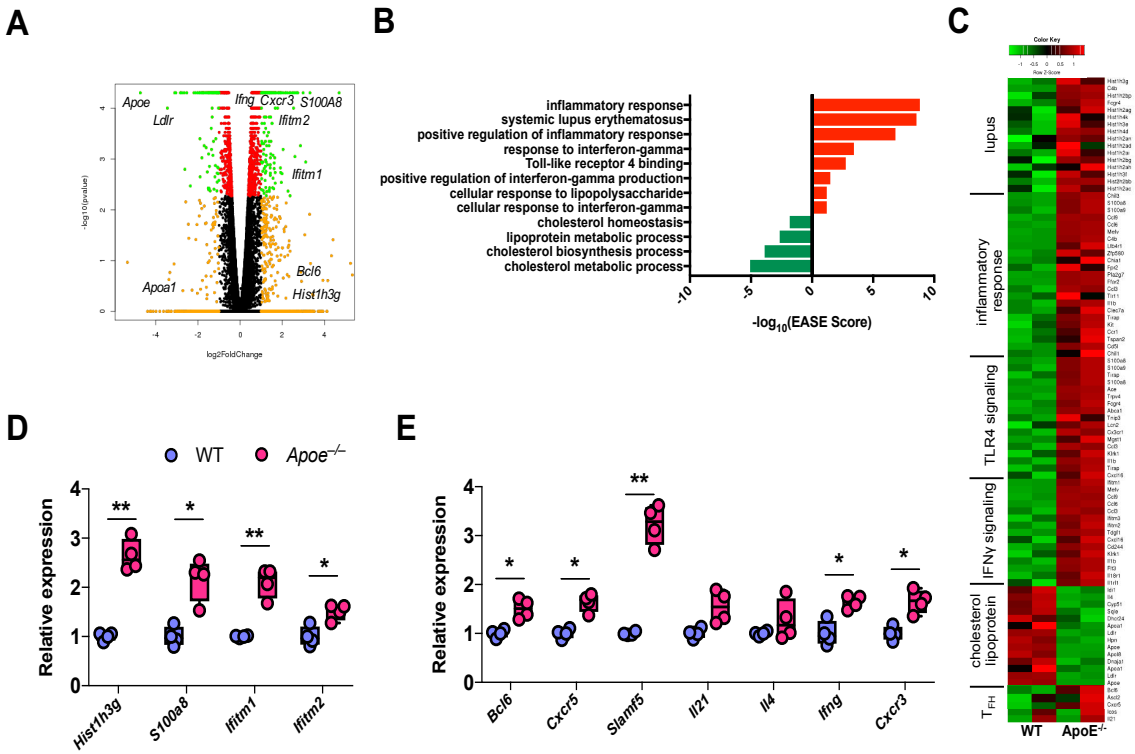

Figure 21. *Transcriptomic analysis of T_{FH} cells isolated from atherogenic mice*
(A-E) T_{FH} cells were isolated as describe in **Figure 19A**.

(A) Gene expression plotted against P values, presented as a volcano plot showing the expression (log2 values) of genes in T_{FH} cells from $Apoe^{-/-}$ mice to their expression in T_{FH} cells from WT mice

(B) Gene-ontology analysis of the mice showing the EASE score (Expression Analysis Systematic Explorer software application) of genes encoding molecules in upregulated (red) or downregulated (green) pathways (left margin).

(C) Heat map of the indicated genes that were differentially expressed subjected to RNA-seq analysis

(D) Quantitative RT- PCR analysis of mRNA from selected genes in T_{FH} cells; results were normalized to those of the control gene *Actb*.

(E) Quantitative RT-PCR analysis of mRNA from T_{FH} cell–related genes in T_{FH} cells; results were normalized to those of the control gene *Actb*

Data are from one experiment representative of three independent experiments.

quantitative RT-PCR (**Figure 21B-D**). Moreover, we also observed that several T_{FH} signature genes including *Bcl6*, *Cxcr5* and *Slamf5* were slightly but significantly upregulated in the T_{FH} cells from the atherogenic mice (**Figure 21E**). In parallel with increased $CXCR3^{+}CCR6^{-}$ T_{FH} cells in $Apoe^{-/-}$ mice, the levels of *Ifng* and *Cxcr3* expression were also upregulated in these T_{FH} cells compared with those from WT mice (**Figure 21E**). As expected, there was a significant reduction in the expression of genes related to cholesterol synthesis and lipoprotein metabolic processes in the $Apoe^{-/-}$ T_{FH} cells (**Figure 21C**). These results together indicate that T_{FH} cells generated in atherogenic environment in vivo exhibited a distinct characteristic including gene expression profile and provided more potent 'help' to B cells to produce IgG2c.

4. IL-27 production by dendritic cells under atherogenic condition

To explore the underlying basis for the augmented autoimmune T_{FH} cell responses in atherogenic mice *in vivo*, the levels of IL-6, IL-27 and IL-12 cytokines, which are known to induce T_{FH} cell differentiation[4, 28], in the sera of WT^{BXD2} and $ApoE^{BXD2}$mice were analyzed. The levels of IL-12p40 (which is a subunit of IL-12 heterodimer cytokine) were comparable in the two groups. By contrast, the levels of IL-27 and IL-6 were significantly higher in $ApoE^{BXD2}$ mice than WT^{BXD2} mice (**Figure 22A**). HFD treatment induced little increase of IL-27 in sera in WT^{BXD2} mice (**Figure 22B**), indicating that the increase of IL-27 in the HFD-fed $ApoE^{BXD2}$ mice was due to atherogenic hyperlipidemia rather than obesity. While both IL-6 and IL-27 showed a positive correlation with the number of T_{FH} cells, IL-27 was found to be more tightly correlated with the numbers of T_{FH} cells (**Figure 22C**). Consistent with the increased IL-27, the levels of *Ebi3* and *Il27* (encoding EBI3 and p28 subunits of IL-27, respectively) and, to a lesser extent, *Il12a* expression were remarkably higher in the DCs from the $ApoE^{BXD2}$ mice than those from the WT^{BXD2} mice (**Figure 23A**). By contrast, the levels of *Il12b*, *Il23a*, and *Il6* appeared to be comparable between the two groups (**Figure 23A**). When these DCs were stimulated with LPS, DCs from the $ApoE^{BXD2}$ secreted more IL-27 and, to a lesser extent, IL-6 than DCs from the WT^{BXD2}, while changes were not observed for IL-12 production (**Figure 23B**).

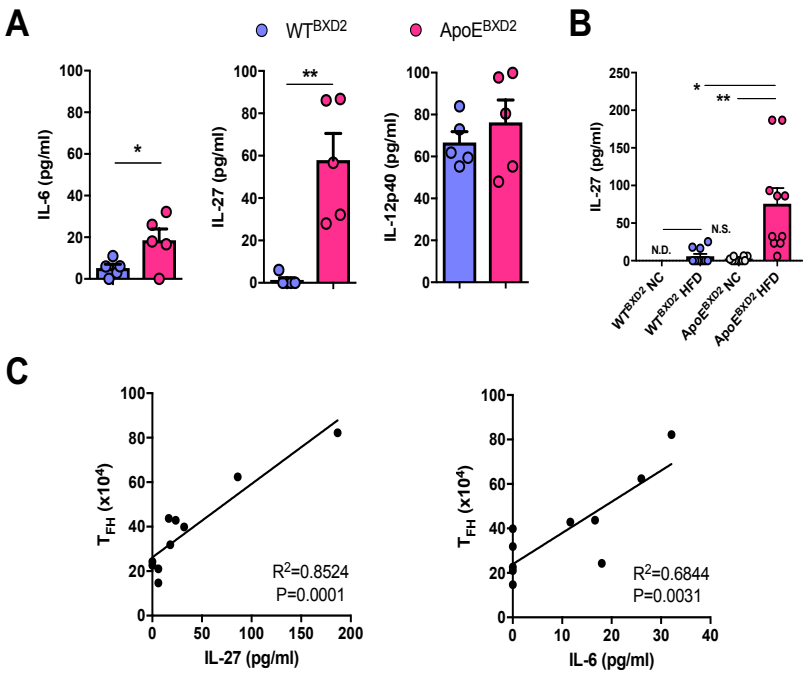

Figure 22. *Elevation of IL-27 cytokine in the serum of atherogenic mice*

(A) Concentration of various cytokines in the serum of WT^{BXD2} and $ApoE^{BXD2}$ mice.

(B) Bone marrow-ablated wild-type or *Apoe*$^{-/-}$ mice were received bone marrow cells from BXD2 mice, were subjected to normal chow (NC) or high fat diet (HFD). Levels of IL-27 in the sera of the indicated mice.

(C) Linear regression analysis between cytokines in the serum and T_{FH}.

Data are from one experiment representative of at least three independent experiments.

When oxidized low-density lipoprotein (oxLDL) were administrated to LPS-stimulated DCs, oxLDL profoundly induced *Ebi3* and *Il27* expression as well as IL-27 protein production, indicating proatherogenic factor, including oxLDL, results IL-27 production by DCs (**Figure 23C, D**).

Conventional DCs can be divided into two populations based on the surface expression of CD11b and CD8α[29]. Notably, we observed a significant increase in the frequency and number of $CD11b^+$ DCs in the spleens of $ApoE^{BXD2}$ mice compared with WT^{BXD2} mice (**Figure 24A**). This DC subset had higher levels of *Ebi3* and *Il27* transcripts than $CD8\alpha^+$ subset, particularly in the atherogenic $ApoE^{BXD2}$ mice (**Figure 24B**). Consistently, the $CD11b^+$ DCs from $ApoE^{BXD2}$mice were far more potent producers of IL-27 upon stimulation with LPS than $CD8\alpha^+$ cells (**Figure 24C**). Among

CD11b$^+$ DCs, the CD4$^-$ subset was more abundant than the CD4$^+$ subset and had higher expression of *Ebi3* than that of the CD4$^+$ subset (**Figure 24D-F**). These results collectively demonstrate that the environment within atherogenic mice not only promoted the accumulation of CD11b$^+$ DCs capable of producing IL-27, but also significantly enhanced the capacity of these DCs to produce IL-27.

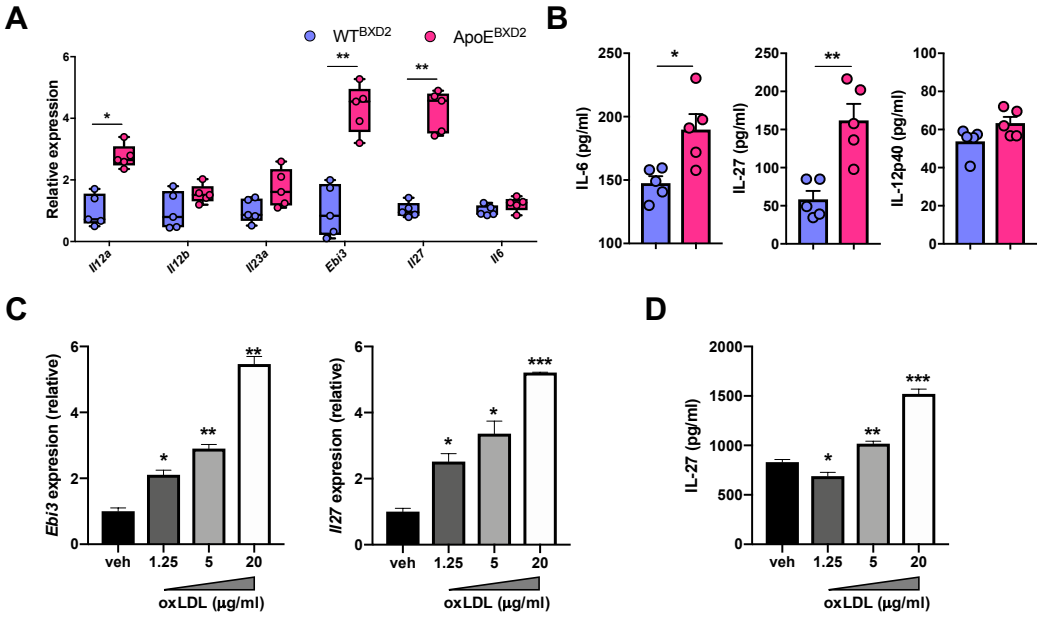

***Figure 23**. IL-27 production by dendritic cells in atherogenic condition*

(A) Quantitative RT-PCR analysis of mRNA in the CD11c$^+$ DCs of the indicated mice; results normalized to those of *Actb*.

(B) Concentration of IL-27 secreted, in the presence of LPS (100 ng/ml), by CD11c$^+$ DCs of the mice.

(C) Quantitative RT-PCR analysis of mRNA in the CD11c$^+$ bone-marrow derived DCs, stimulated with LPS (100 ng/ml) in the presence of increasing concentration of oxLDL; results normalized to those of *Actb*.

(D) Concentration of IL-27 secreted by CD11c$^+$ bone-marrow derived DCs, stimulated with LPS (100 ng/ml) in the presence of increasing concentration of oxLDL.

Data are from one experiment representative of at least three independent experiments.

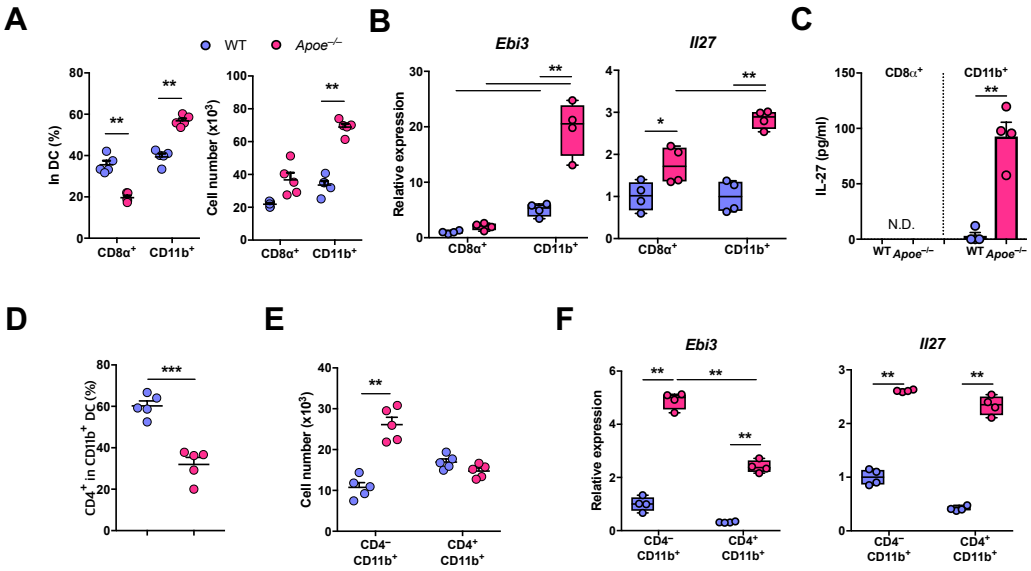

Figure 24. *Dendritic cell subset analysis in atherogenic mice*

(A) Frequency (assessed by flow cytometry) and absolute number of DC subsets in the indicated mice.

(B) Quantitative RT-PCR analysis of *Ebi3* and *Il27* mRNA in splenocytes obtained from the mice, then sorted by flow cytometry into subsets (horizontal axis); results normalized to those of *Actb*.
(C) Concentration of IL-27 secreted, in the presence of LPS (100 ng/ml), by various subsets of DCs in the indicated mice.

(D, E) Frequency of $CD4^+$ cells among $CD11b^+$ DCs (assessed by flow cytometry) (D), and number of $CD4^-CD11b^+$ or $CD4^+CD11b^+$ DCs (E), in the mice.

(F) Quantitative RT-PCR analysis of *Ebi3* and *Il27* mRNA in $CD4^-CD11b^+$ and $CD4^+CD11b^+$ DCs sorted by flow cytometry from the mice; results normalized to those of *Actb*.

Data are from one experiment representative of three independent experiments.

5. Lipid metabolism of IL-27 production by dendritic cells

To determine the molecular mechanism by which the atherogenic environment triggered the production of IL-27 from DCs, energy metabolism of DCs were analyzed. Analysis of energy metabolism (by measurement of the oxygen-consumption rate and extracellular acidification rate) revealed that DCs from HFD-fed *Apoe*$^{-/-}$ mice exhibited a significantly higher glycolysis, glycolytic capacity and respiratory reserve capacity than that of DCs from HFD-fed WT mice indicative of robust upregulation of energy-generating pathways in DCs exposed to an atherogenic environment (**Figure 25A-E**).

Moreover, BODIPY-staining analysis showed that the intracellular lipid content was greater in DCs from ApoE^{BXD2} mice than in those from WT mice, a result that was not observed for T cells and B cells (**Figure 26A, B**)

To further characterize DCs generated in hyperlipidemic condition, transcriptome analysis of these cells was performed by RNA sequencing (RNA-seq) on the DCs isolated from HFD-fed WT and *Apoe*$^{-/-}$ mice. Ingenuity Pathway Analysis (IPA) revealed alteration in lipid-activated transcription factors pathway in DCs, with the most significant changes in LXR pathway (**Figure 27A, B**). The abundance of *Nr1h2*

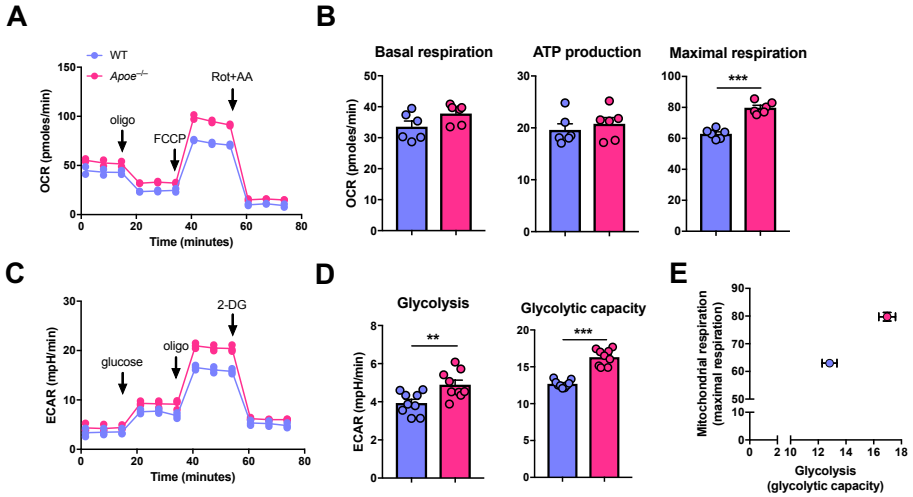

Figure 25. *Altered energy metabolism in DCs generated in hyperlipidemic condition*

(A-E) CD11c^{+} dendritic cells were isolated from the indicated mice and were analyzed for OCR profile (A), basal respiration, ATP production, and maximal respiration (B), OCR profile (C), and glycolysis, glycolytic capacity (D). Energy map of dendritic cells isolated from the indicated mice (E).

Data are from one experiment representative of three independent experiments.

transcripts (which encode LXRβ) and LXRβ protein, but not that of *Nr1h3* transcripts (which encode LXRα), was significantly lower in DCs from *Apoe*$^{-/-}$ mice than in those from WT mice (**Figure 27C-E**). To determine if the reduced expression of LXRβ contributed to the increased production of IL-27 in athero- genic mice, the production of IL-27 by DCs stimulated were measured in the presence of the LXR agonist GW396524. GW3965 significantly reduced the expression of *Ebi3* and *Il27* (**Figure 27F**) and consequent IL-27 protein secretion (**Figure 27G**), suggesting that restoration of LXRβ activity diminished that increase in the production of IL-27 by DCs from atherogenic mice.

LXRβ-deficient mice (*Nr1h2*$^{-/-}$) exhibited similar dendritic cell distribution pattern to *Apoe*$^{-/-}$ mice; an increase in the frequency of CD11b^{+} and CD4^{-} DCs and higher levels of *Ebi3* and *Il27* transcripts (**Figure 28A-C**). When LXR agonist GW3965 was administrated to LPS-stimulated wild type DCs, GW3965 profoundly diminished *Ebi3* and *Il27* expression as seen in dendritic cells from hyperlipidemic mice (**Figure 28D**), suggesting that LXR regulates IL-27 production by dendritic cells not only under atherogenic environment but also physiological condition. Deletion of *Tlr4* did not affect LXR-mediated suppression of IL-27, but inhibition of Mer tyrosin kinase (MERTK), which is a downstream molecule of LXR, induced *Ebi3* and *Il27* transcripts, which suggesting that LXR regulates IL-27 production in TLR4-independent and MERTK-dependent manner (**Figure 29A,B**).

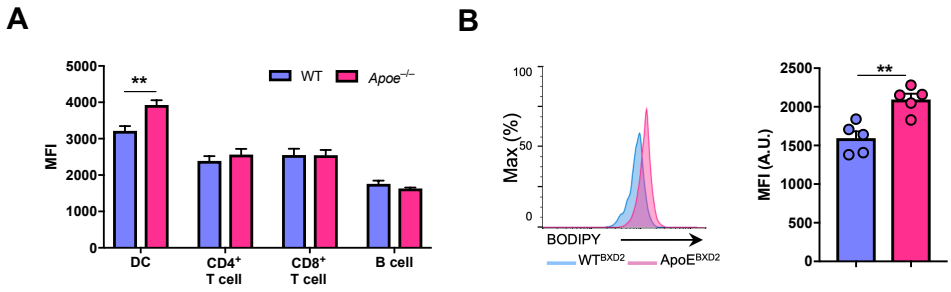

Figure 26. *Lipid accumulation in dendritic cells generated in atherogenic condition*

(A) Flow cytometry of each cell type obtained from WT and *Apoe*$^{-/-}$ mice and stained with the fluorescent dye BODIPY.

(B) BODIPY staining of DCs from WT^{BXD2} and ApoE^{BXD2} (left), and mean fluorescent intensity of BODIPY in those cells (right).

Data are from one experiment representative of at least three independent experiments.

A

Top Tox Lists		
Name	p-value	Overlap
LXR/RXR Activation	3.43E-08	10.6 % 13/123
Persistent Renal Ischemia-Reperfusion Injury (Mouse)	4.26E-06	20.0 % 6/30
LPS/IL-1 Mediated Inhibition of RXR Function	1.08E-04	5.1 % 13/254
Genes associated with Chronic Allograft Nephropathy (Human)	2.25E-04	19.0 % 4/21
FXR/RXR Activation	5.62E-04	6.3 % 8/126

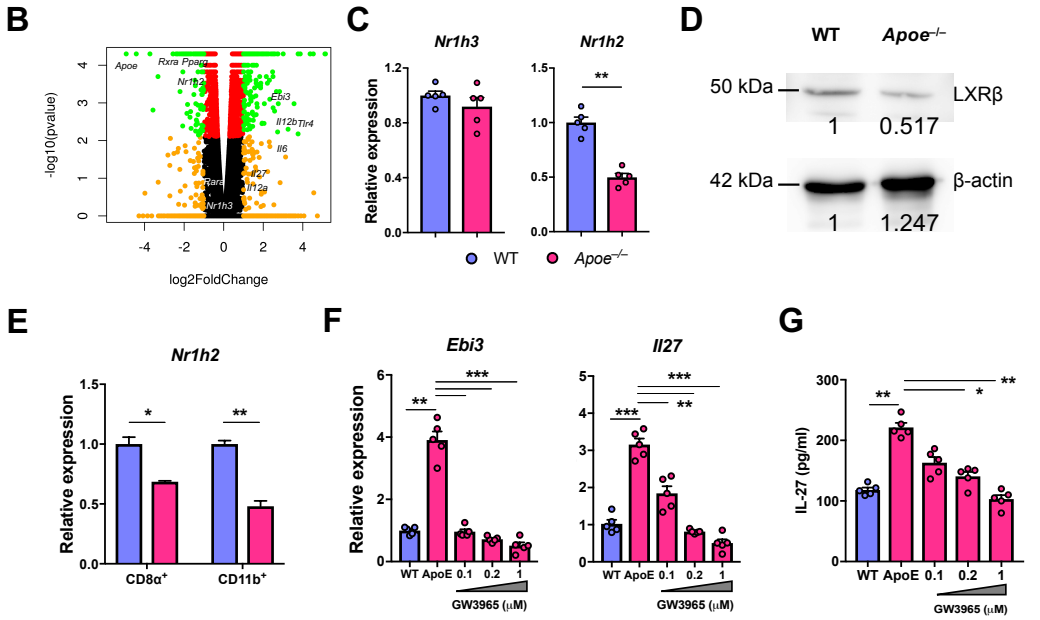

Figure 27. *Regulation of IL-27 production by LXR*

(A, B) CD11c^{+} DCs were isolated from WT and *Apoe*$^{-/-}$ mice, and RNA-seq and Ingenuity Pathway Analysis (IPA) were performed.

(A) IPA analysis result.

(B) Volcano plot of showing the expression (log2 values) of genes in DCs from *Apoe*$^{-/-}$ mice to their expression in DCs from WT mice.

(C) Quantitative RT-PCR analysis of *Nr1h3* and *Nr1h2* mRNA in CD11c^{+} DCs isolated from the spleen of WT or *Apoe*$^{-/-}$ mice; results normalized to those of *Actb*.

(D) The expression of LXRβ was examined by Immunoblot. Quantified values of the band intensities are presented at the bottom of each blot.

(E) Quantitative RT-PCR analysis of *Nr1h2* mRNA in the indicated DC subsets; results normalized to those of *Actb*.

(F) Quantitative RT-PCR analysis of *Ebi3* and *Il27* mRNA in CD11c^{+} DCs, stimulated with LPS (100 ng/ml) in the presence of increasing concentrations of GW3965; results normalized to those of *Actb*.

(G) Concentration of IL-27 produced by CD11c^{+}, stimulated with LPS (100 ng/ml) in the presence of increasing concentrations of GW3965.

Data are from one experiment representative of three independent experiments.

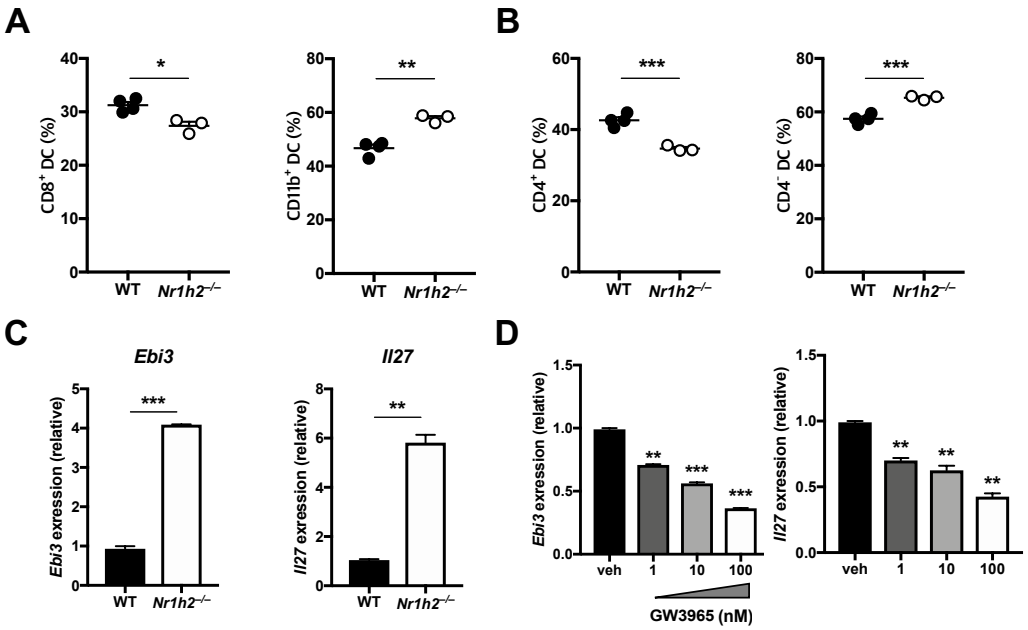

Figure 28. *Regulation of dendritic cells by LXRβ*

(A) Frequency (assessed by flow cytometry) of DC subsets in the indicated mice.

(B) Frequency of $CD4^+$ cells among $CD11b^+$ DCs (assessed by flow cytometry) in the mice.

(C) Quantitative RT-PCR analysis of *Ebi3* and *Il27* mRNA in splenocytes obtained from the mice; results normalized to those of *Actb*.

(D) Quantitative RT-PCR analysis of *Ebi3* and *Il27* mRNA in $CD11c^+$ bone-marrow derived DCs, stimulated with LPS (100 ng/ml) in the presence of increasing concentrations of GW3965; results normalized to those of *Actb*.

Data are from one experiment representative of at least three independent experiments.

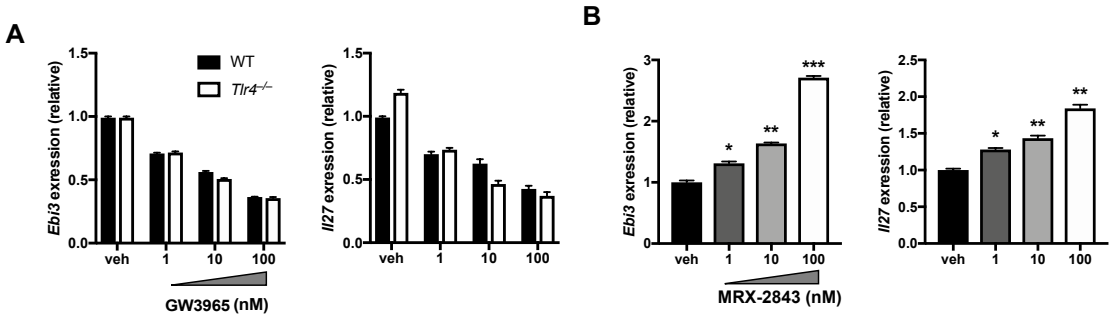

Figure 29. *TLR4-independent regulation of IL-27 by LXR*

(A) Quantitative RT-PCR analysis of *Ebi3* and *Il27* mRNA in CD11c^{+} bone-marrow derived DCs from WT and *Tlr4*$^{-/-}$ mice, stimulated with LPS (100 ng/ml) in the presence of increasing concentrations of GW3965; results normalized to those of *Actb*.

(B) Quantitative RT-PCR analysis of *Ebi3* and *Il27* mRNA in CD11c^{+} bone-marrow derived DCs, stimulated with LPS (100 ng/ml) in the presence of increasing concentrations of MRX-2843; results normalized to those of *Actb*.

Data are from one experiment representative of two independent experiments.

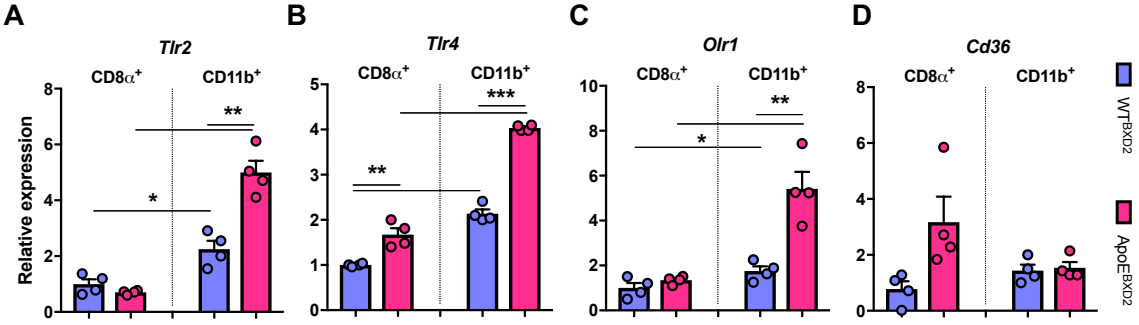

Figure 30. *Altered pattern-recognition receptor expression in dendritic cells generated in atherogenic condition*

(A-D) Quantitative RT-PCR analysis of *Tlr2* (A), *Tlr4* (B), *Olr1* (C), and *Cd36* (D) in the indicated DC subsets isolated from the spleen of WT^{BXD2} or ApoE^{BXD2} mice; results normalized to those of *Actb*.

Data are from one experiment representative of at least three independent experiments.

OxLDL increased IL-27 production from DCs (**Figure 23C,D**), and this hallmark of atherogenic dyslipidemia can be recognized by DCs and macrophages through TLR2, TLR4, LOX-1 and CD36[30, 31]. The expression patterns of these receptors on dendritic cells under hyperlipidemic condition were analyzed. DCs from $ApoE^{BXD2}$ expressed higher levels of *Tlr2*, *Tlr4*, *Olr1* (encoding LOX1) compared with those from WT^{BXD2}, particularly in $CD11b^{+}$ subsets (**Figure 30A-D**). Since TLR4 is well-known to stimulate DCs to produce proinflammatory cytokines, TLR4 might also be required for the production of IL-27 by dendritic cells under hyperlipidemia. To test the idea, oxLDL were administrated to WT or TLR4-deficient DCs in vitro, and induction of IL-27 was not observed in TLR4-deficient DCs (**Figure 31A**).

To further demonstrate the role of TLR4 for IL-27 production and germinal center reactions under atherogenic conditions in vivo, bone marrow chimeric mice were generated by transferring bone marrow cells of WT or TLR4-deficient mice into bone marrow-ablated WT or ApoE-deficient mice (WT^{WT}, $ApoE^{WT}$, and $ApoE^{TLR4}$, respectively). After reconstitution, the recipient mice were maintained on HFD (**Figure 31B**). Increased of IL-6 and IL-27 in the sera of atherogenic mice was no longer observed in the sera of $ApoE^{TLR4}$, indicating an essential role of TLR4 for the increased production of IL-6 and IL-27 in the atherogenic mice. manner, which was significantly attenuated in the DCs from $ApoE^{TLR4}$ mice (**Figure 31C**). Moreover, increased serum levels of total IgG and IgG2c in atherogenic condition was undistinguishable between WT^{WT} mice and $ApoE^{TLR4}$ mice (**Figure 31D**).

When these mice were immunized with NP-OVA in CFA, the levels of NP-specific total IgG and IgG2c in the $ApoE^{TLR4}$ mice were higher than those in the WT^{WT} mice, they were significantly lower than those in the $ApoE^{WT}$ mice (**Figure 31E**). Also, the frequencies of GC B, plasma, and T_{FH} cells in the draining LNs were all significantly higher in the $ApoE^{WT}$ mice than those of the WT^{WT} mice, which was diminished to the levels of WT^{WT} mice in the $ApoE^{TLR4}$ mice (**Figure 31F**). Oxidized LDL substantially induced the production of IL-6 and IL-27, but not that of IL-12p40, by DCs from the $ApoE^{WT}$ mice, in a dose-dependent manner, relative to such production by DCs from the

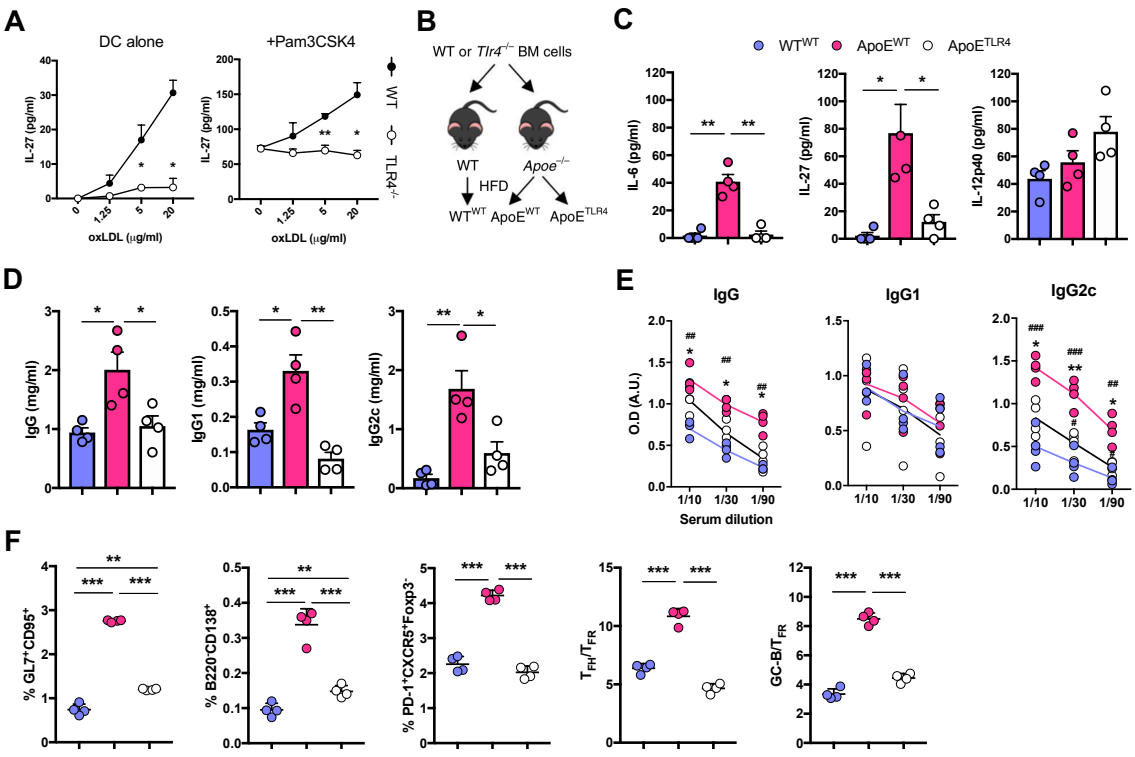

Figure 31. *TLR4-mediated IL-27 production under atherogenic condition in vivo*

(A) Concentration of IL-27 secreted by $CD11c^+$ bone-marrow derived DCs from WT and *Tlr4*$^{-/-}$ mice, in the presence of increasing concentration of oxLDL, stimulated with Pam3CSK4 (200 ng/ml) (right) or not (left).

(B) Experimental procedure: WT mice and *Apoe*$^{-/-}$ mice in which the bone marrow was ablated were given intravenous transfer of bone marrow cells from WT of *Tlr4*$^{-/-}$ mice and were fed an HFD.

(C) Concentration of various cytokines in the serum of the indicated mice.

(D) ELISA of total IgG, IgG1 and IgG2c antibodies in the serum of the mice.

(E, F) The mice described on **Figure 31B** were immunized with KLH in CFA and analyzed on day 7.

(E) ELISA of KLH-specific total IgG, IgG1 and IgG2c antibodies in the serum of the indicated mice.
(F) Frequency of $GL7^+CD95^+$ cells (GC B cells), and $B220^-CD138^+$ cells (plasma cells), and PD- $1^+CXCR5^+Foxp3^-$ cells (T_{FH} cells) as well as the ratio of T_{FH} cells to T_{FR} cells (T_{FH}/T_{FR}) and of GC B cells to T_{FR} cells (GC B/T_{FR}) among lymphocytes from the mice, assessed by flow cytometry.

Data are from one experiment representative of three independent experiments.

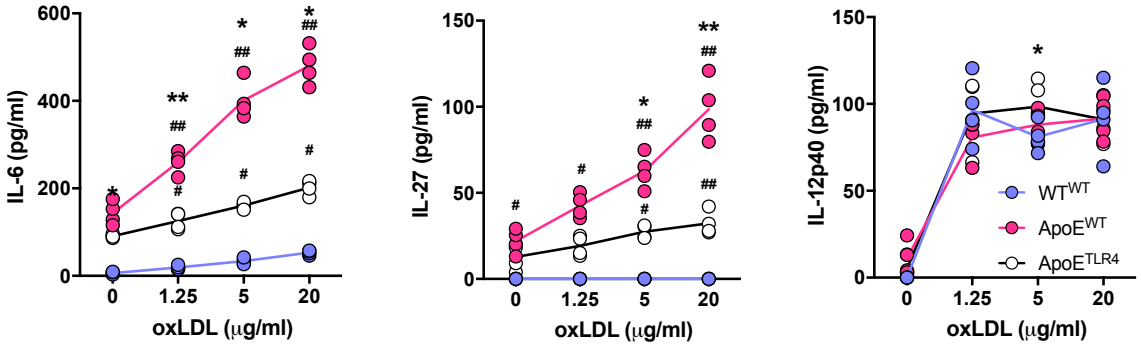

Figure 32. *TLR4-mediated IL-27 production by dendritic cells*

Concentration of various cytokines produced by $CD11c^+$ isolate from indicated mice, stimulated with increasing concentrations of oxLDL.

Data are from one experiment representative of three independent experiments.

WT^{WT} mice, and this was significantly attenuated in the DCs from $ApoE^{TLR4}$ mice, relative to that in DCs from $ApoE^{WT}$ mice (**Figure 32**). Altogether, these results demonstrate an essential role of lipid metabolism for inducing the increase IL-27 production and for the enhanced T_{FH} cells and germinal center reactions under atherogenic conditions *in vivo*.

6. Role of IL-27 in germinal center reaction under atherogenic condition

The profound increase in the level of IL-27 observed in the HFD-fed $ApoE^{BXD2}$, $LDLR^{BXD2}$ and *Apoe*$^{-/-}$ mice lead to hypothesis that IL-27 plays a crucial role in enhanced germinal center reactions and antibody production, particularly IgG2c, as well as in the generation of highly pathogenic T_{FH} cells. To test this hypothesis, *Apoe*$^{-/-}$ mice lacking *Ebi3* (*Ebi3*$^{-/-}$*Apoe*$^{-/-}$; dKO) were generated and subjected on HFD. As expected, IL-27 was absent in the dKO mice whereas the levels of IL-6 and IL-12p40 were marginally affected by deletion of IL-27Ebi3 (**Figure 33A**). Interestingly, the levels of IgG autoantibodies against dsDNA, particularly IgG2c isotype, that were significantly higher in *Apoe*$^{-/-}$ mice were diminished in dKO mice (**Figure 33B**). When these mice

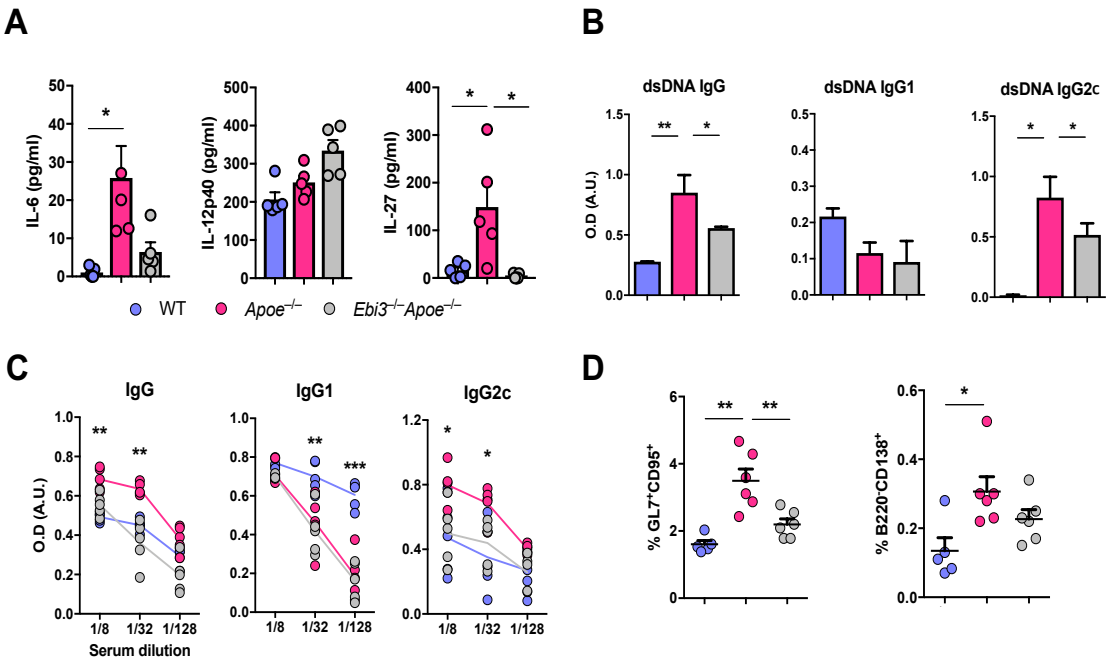

Figure 33. *Regulation of germinal center reactions by deletion of IL-27EBI3*

(A-D) WT, *Apoe*$^{-/-}$, and *Ebi3*$^{-/-}$*Apoe*$^{-/-}$ mice were fed an HFD for 4 weeks before being immunized with OVA-NP in CFA.

(A) Concentration of various cytokines in the serum of the indicated mice.

(B) ELISA of autoreactive IgG-subclass autoantibodies to dsDNA in the serum of the mice.

(C) ELISA of NP-specific total IgG, IgG1 and IgG2c antibodies in the serum of the indicated mice.

(D) Frequency of GL7^{+}CD95^{+} cells (GC B cells) and B220^{-}CD138^{+} cells (plasma cells) among lymphocytes from the mice, assessed by flow cytometry.

Data are from one experiment representative of at least three independent experiments.

were immunized with OVA-NP in CFA, the levels of NP-specific IgG and IgG2c antibodies that were elevated in *Apoe*$^{-/-}$ mice were significantly diminished to the levels of WT mice in the dKO mice, while the levels of IgG1 were not affected in the dKO (**Figure 33C**). Moreover, compared with *Apoe*$^{-/-}$ mice, the frequencies of GC B and T_{FH} cells, not as much for plasma cells, in the dKO mice was almost completely decreased to the levels of WT mice (**Figure 33D & Figure 34A**). To further interrogate the role of IL-27 on the T_{FH} function in atherogenic condition *in vivo*, T_{FH} cells from WT, *Apoe*$^{-/-}$, and dKO mice were co-cultured with naïve B cells, and T_{FH} cells from the dKO mice, unlike

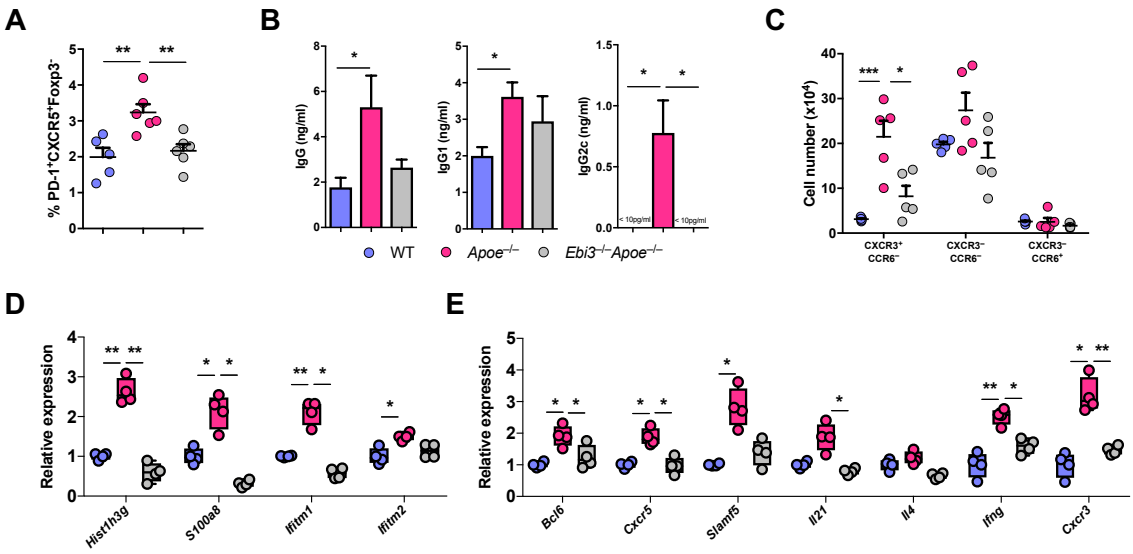

Figure 34. *Effects of IL-27 on pathogenicity of T_{FH} cells*

(A) Frequency of PD- $1^{+}CXCR5^{+}Foxp3^{-}$ cells (T_{FH} cells) ong lymphocytes from the indicated mice, assessed by flow cytometry.

(B) ELISA of total IgG, IgG1 and IgG2c in supernatants of T_{FH} cells from the indicated mice and naïve B cells co-cultured for 7 days in the presence of anti-CD3 and anti-IgM.

(C) Number of each T_{FH} cell subsets in the mice.

(D) Quantitative RT- PCR analysis of mRNA from selected genes in T_{FH} cells; results were normalized to those of the control gene *Actb*.

(E) Quantitative RT-PCR analysis of mRNA from T_{FH} cell–related genes in T_{FH} cells; results were normalized to those of the control gene *Actb*.

Data are from one experiment representative of at least three independent experiments.

those from *Apoe*$^{-/-}$ mice, failed to trigger IgG2c production from naïve B cells *in vitro* (**Figure 34B**). Compared with *Apoe*$^{-/-}$ mice, the number of $CXCR3^{+}CCR6^{-}$ T_{FH} cells was significantly diminished in the dKO mice (**Figure 34C**). Gene expression related to inflammatory responses, SLE, and T_{FH} cell programs on FACS-sorted T_{FH} cells from WT, *Apoe*$^{-/-}$, and dKO mice were analyzed. Levels of gene expression that were increased in *Apoe*$^{-/-}$ mice were significantly diminished to the levels of WT in the dKO mice (**Figure 34D, E**). To demonstrate the role of IL-27 more definitively, *Apoe*$^{-/-}$ mice in which the bone marrow was ablated were given adoptive transfer of WT or cytokine receptor IL-27R-deficient (*Il27ra*$^{-/-}$) mice bone marrow cells before being fed an HFD, and the

recipient mice were immunized with KLH in CFA (**Figure 35A**). A significantly lower abundance of anti- KLH IgG, especially IgG2c, and TFH cells, particularly the CXCR3+ subset, were found in the recipients of *Il27ra*$^{-/-}$ bone marrow than in those

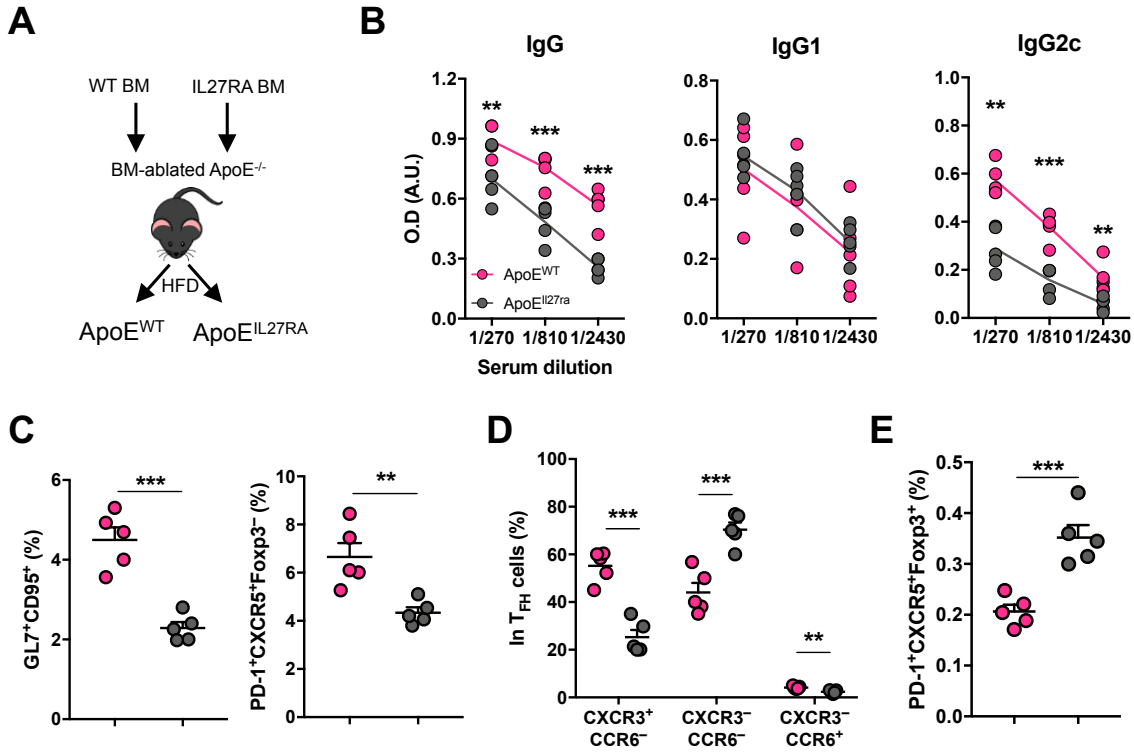

Figure 35. *Effects of IL-27 signaling on germinal center reaction*

(A) Experimental procedure: *Apoe*$^{-/-}$ mice in which the bone marrow was ablated were given intravenous transfer of bone marrow cells WT or *Il27ra*$^{-/-}$ mice and were fed an HFD.

(B-E) ApoE^{WT} and ApoE^{IL27RA} mice were immunized with KLH in CFA and analyzed on day 7.

(B) ELISA of KLH-specific total IgG, IgG1 and IgG2c antibodies in the serum of the indicated mice.

(C-E) Frequency of GL7^{+}CD95^{+} cells (GC B cells), B220^{-}CD138^{+} cells (plasma cells) (C), each TFH cell subsets (D), and Foxp3^{+} T_{FH} cells (T_{FR} cells) (E) among lymphocytes from the mice, assessed by flow cytometry.

Data are from one experiment representative of three independent experiments.

given WT bone marrow cells, while the frequency of TFR cells was higher in the recipients of *Il27ra*$^{-/-}$ bone marrow (**Figure 35B-E**).

Injection of anti-IL-6 also significantly diminished KLH-specific antibody responses, frequencies of T_{FH} cells, GC B cells and plasma cells in *Apoe*$^{-/-}$ mice

immunized with KLH in CFA (**Figure 36A-C**). Anti-IL-6 also decreased the frequency of T_H17 cells, but not that of T_H1 cells (**Figure 36D**). However, unlike the blockade of IL-27 signaling, treatment with anti-IL-6 decreased not only the production of IgG2c and the number of $CXCR3^+$ T_{FH} cells but also the production of IgG1 and the number of $CXCR3^-$ T_{FH} cells (**Figure 36B, E**).

Stimulation with IL-6 or IL-27 induces the differentiation of naive $CD4^+$ T cells into IL-21-producing 'T_{FH}-like cells' *in vitro*. When naive OT-II $CD4^+$ T cells were stimulated with splenocytes in the presence of $Ova_{323-335}$, addition of IL-27 induced IL-21 and IFN-γ from the OT-II T cells, while IL-6 induced IL-21 but not IFN-γ (**Figure 37A**). IL-6 and IL-27 appeared to synergistically trigger IL-21 and IFN-γ from the OT-II T cells.

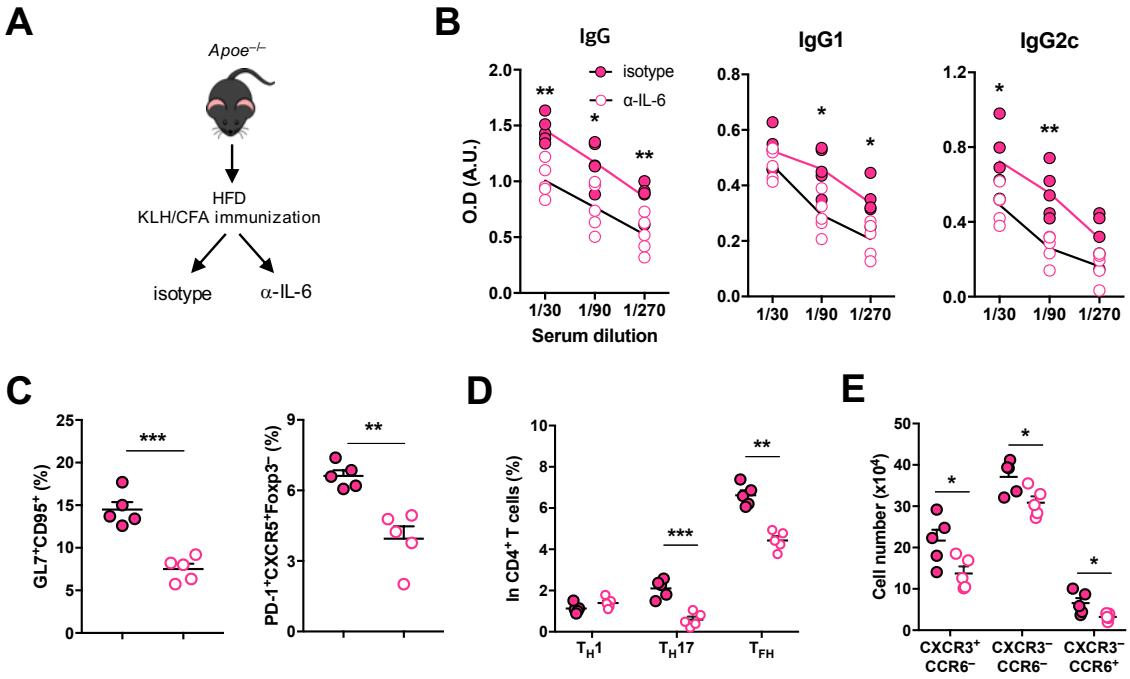

Figure 36. *Indispensable role of IL-6 in germinal center reaction*

(A) Experimental procedure: *Apoe*$^{-/-}$ mice were fed with HFD for four weeks, immunized with KLH and analyzed after seven days. Each group of mice were injected with control IgG or anti-IL-6 antibody intraperitoneally every other day.

(B) Levels of KLH-specific antibodies in the sera of the indicated mice.

(C-E) Frequency of $GL7^+CD95^+$ cells (GC B cells), $B220^-CD138^+$ cells (plasma cells) (C) and helper T cell subsets (D), and number of each TFH cell subsets (E) among lymphocytes from the mice, assessed by flow cytometry.

Data are from one experiment representative of three independent experiments.

When these cells were co-cultured with naive B cells in the presence of anti-CD3 and anti-IgM, OT-II T cells that previously stimulated with IL-6 and IL-27 were the most potent in inducing both IgG1 and IgG2c production compared with OT-II T cells stimulated with each cytokine alone (**Figure 37B**).

Since IL-27 induces signaling via the transducers STAT1 and STAT3[32], the role of these STAT proteins in the enhanced T_{FH} cell responses in atherogenic mice was assessed. Mixed–bone marrow chimeras were generated by transferring a 1:1 bone marrow cell mixture of WT (CD45.1$^+$) and either *Stat1*$^{-/-}$or conditional deletion of *Stat3* in CD4$^+$ T cells (CD4^{Stat3} mice) (all CD45.2$^+$) into bone marrow-ablated *Apoe*$^{-/-}$ mice, then fed the recipients an HFD and subsequently immunized them with KLH in CFA (**Figure 38A**). The frequency of T_{FH} cells was lower among STAT1- or STAT3-deficient CD4$^+$ T cells than among their respective WT counterparts (**Figure 38B**). Significant reduction in the CXCR3$^+$ T_{FH} subset were found among STAT1-deficient T_{FH} cells but not among STAT3-deficient T_{FH} cells (**Figure 38C**). When CXCR3$^-$ T_{FH} cells sorted by flow cytometry were stimulated with IL-27, STAT1-deficient T cells failed to induce the expression of *Cxcr3* or *Ifng*, while STAT3-defient T cells showed no defect in inducing

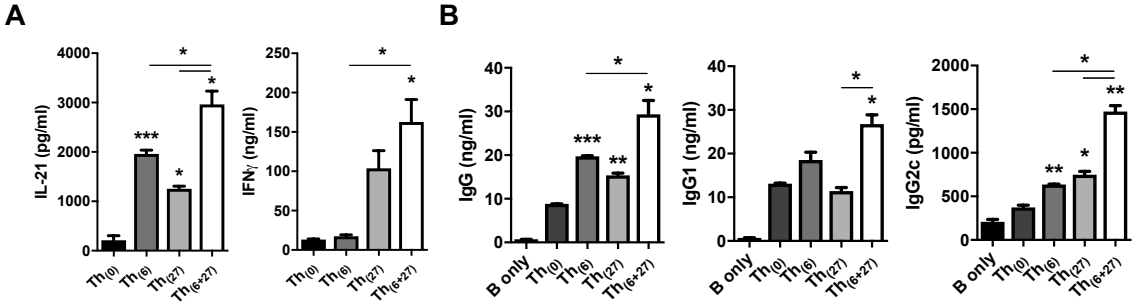

***Figure 37**. Synergistic effects of IL-6 and IL-27 on IL-21-producing cell*

(A, B) Naive OT-II T cells were co-cultured with MMC-treated splenocytes in the presence of OVA-peptide and indicated cytokines for three days. The cells were re-stimulated with anti-CD3 for 24 hours (A), or co-cultured with naïve B cells for seven days (B).

(A) Cytokine levels from cultured supernatant.

(B) ELISA of total IgG, IgG1 and IgG2c in supernatants of co-cultured.

Data are from one experiment representative of at least three independent experiments.

those genes but failed to induce *Il21* (**Figure 39A-C**). These results together demonstrated an essential role for IL-27 in the differentiation of pathogenic T_{FH} cell, particularly CXCR3^{+} T_{FH} cells, and subsequent GC reactions in atherogenic mice.

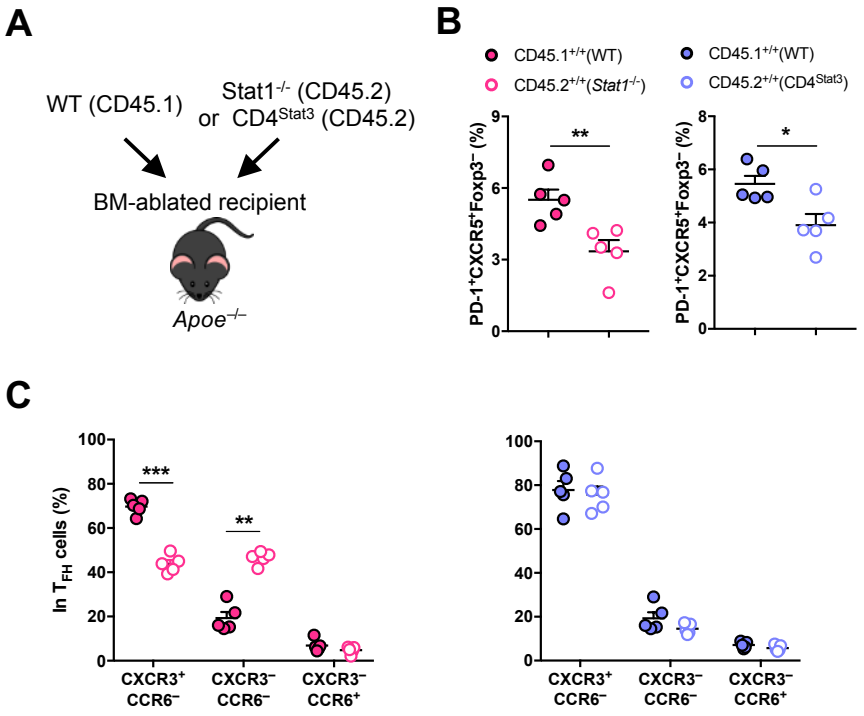

Figure 38. *STAT1 and STAT3 regulation in T_{FH} cells generated in atherogenic condition*

(A) Experimental procedure: *Apoe*$^{-/-}$ mice in which the bone marrow was ablated, that were reconstituted by intravenous transfer of mixture of bone marrow cells from congenic WT mice or *Stat1*$^{-/-}$ mice or CD4^{Stat3} mice.

(B, C) Frequency of T_{FH} cells (B) and various subsets of T_{FH} cells (C) among lymphocytes from the indicated mice, assessed by flow cytometry.

Data are from one experiment representative of three independent experiments.

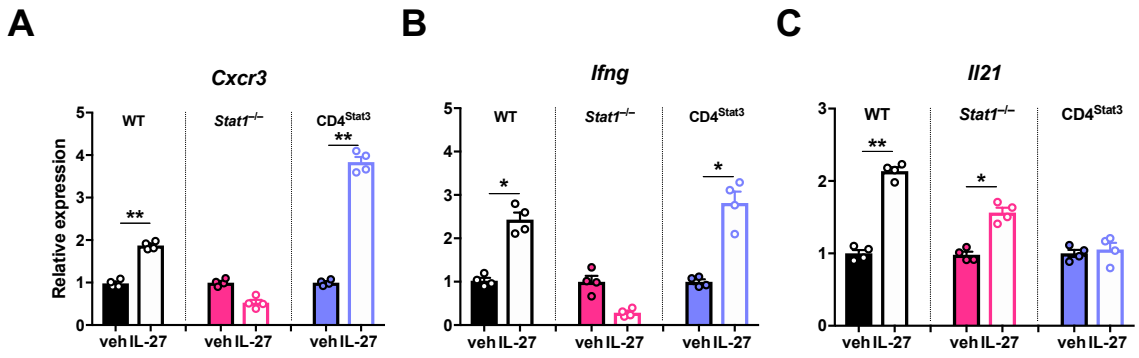

Figure 39. *Regulation of CXCR3^{+} T_{FH} cells by IL-27*

(A-C) Quantitative RT-PCR analysis of *Cxcr3* (A), *Ifng* (B) and *Il21* (C) mRNA in CXCR3^{-} T_{FH} cells isolated from WT, *Stat1*$^{-/-}$ or CD4^{Stat3} mice and stimulated with IL-27; results normalized to those of *Actb*.

Data are from one experiment representative of three independent experiments.

7. Analysis of human patients with hyperlipidemia

To demonstrate clinical relevance of our findings, plasma samples of a cohort in patients with hypercholesterolemia or in healthy individuals were analyzed (**Figure 40A**). The plasma concentration of IL-6 was comparable between the two groups, the level of IL-27 was significantly higher in the patients that healthy controls (**Figure 40B**). Moreover, the plasma from the patients exhibited slightly, but significantly, higher levels of IgG autoantibodies to dsDNA (**Figure 40C**). Levels of total IgG were also significantly increased, presumably due to the increases of IgG1 and IgG3, which are homologues to mouse IgG2 subclasses (**Figure 40D**)[33]. These results demonstrate that patients with hypercholesterolemia exhibited augmented levels of IL-27 associated with increase in the levels of IgG antibody, particularly IgG1 and IgG3.

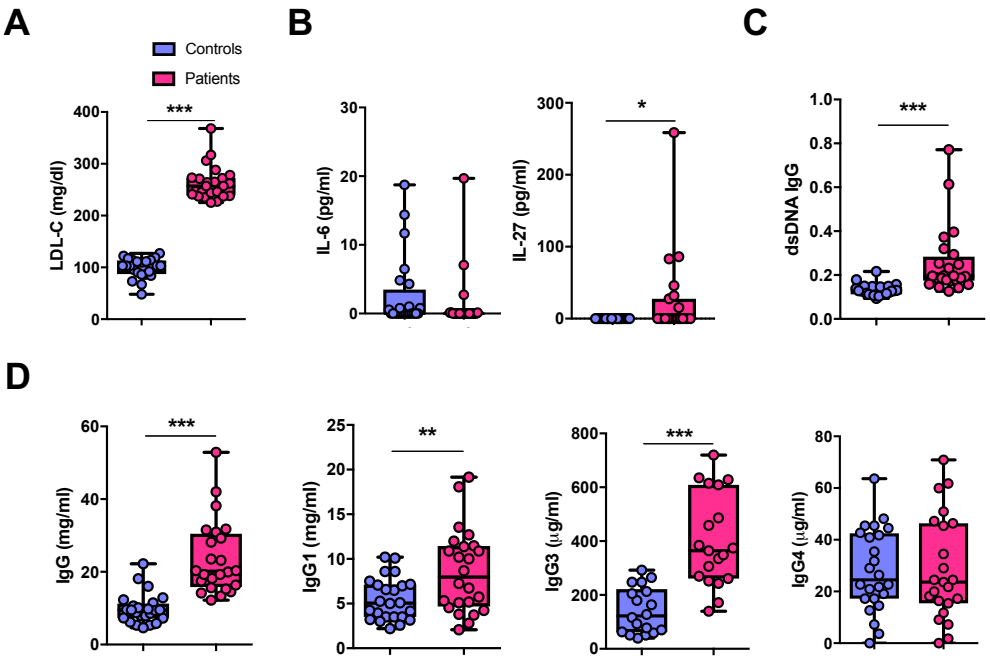

***Figure 38**. Increased autoantibodies and IL-27 in patients with hypercholesterolemia*

(A) Concentration of LDL cholesterol (LDL-c) in the plasma of healthy donors (Controls) or patients with hypercholesterolemia (Patients).

(B) Concentration of cytokines in the plasma of subjects.

(C) Level of autoreactive IgG antibodies to dsDNA in subjects.

(D) Concentration of total IgG and IgG-subclass antibodies in subjects.

V. Discussion

In this study, the role of T_{FH} cells during the pathogenesis of atherosclerosis-related autoimmune diseases, particularly SLE, was demonstrated. Aside from the key role of hyperlipidemia and lipid metabolism in the pathogenesis of atherosclerosis, several clinical implications and studies suggest a pathogenic role of these conditions in autoimmune diseases including lupus. Given the fact that both cardiovascular and autoimmune diseases are leading causes of death and disability world-widely, it is important to elucidate cross-regulatory mechanisms by which those diseases are progressed. Using in vivo animal models of atherosclerosis and autoimmune lupus, it has been demonstrated that hyperlipidemic conditions significantly increased the production of autoantibodies, particularly IgG2c, and the severity of SLE by augmenting T_{FH} cell responses. These findings unveil a novel mechanism by which atherogenic dyslipidemia promotes T_{FH} cell responses and GC reactions against lupus-associated self-antigens as well as exogenous antigens via IL-27 in vivo (**Figure 41**)[34].

1. T_{FH} cell differentiation regulated by IL-27

T_{FH} cell differentiation is initiated by IL-6, IL-12 and IL-27 cytokine by inducing IL-21 production by $CD4^+$ T cells. Originally, IL-27 is known to induce T_H1 responses via STAT1 regulation. Recent findings suggested that IL-27 also could promote T_{FH} cell differentiation and germinal center reactions STAT3/STAT1 activation[28]. Through analysis of wild-type or *Apoe*$^{-/-}$ mice recipients of lupus-prone BXD2 bone marrow cells as well as human cohorts, the serum level of IL-27 was significantly increased in the patients with hypercholesterolemia and the atherogenic mice. As a proof, blockade of IL-27 signal in atherogenic mice significantly reduced generation of T_{FH} cells and consequent GC reactions.

Studies with T cells deficient in STAT1 or STAT3 revealed that STAT1 is required for the expression of *Cxcr3* and *Ifng* by T_{FH} cells in atherogenic mice in a cell-intrinsic manner. IL-6 production was also increased in atherogenic mice; however, increased IL-27, rather than IL-6, might account for the augmentation of T_{FH} cell and GC reactions based on (i) blockade of IL-27 signal specifically reduced the features of germinal center reactions in atherogenic mice, (ii) neutralization of IL-6 non-specifically reduced overall germinal center reactions including $CXCR3^-$ T_{FH} cell and IgG1

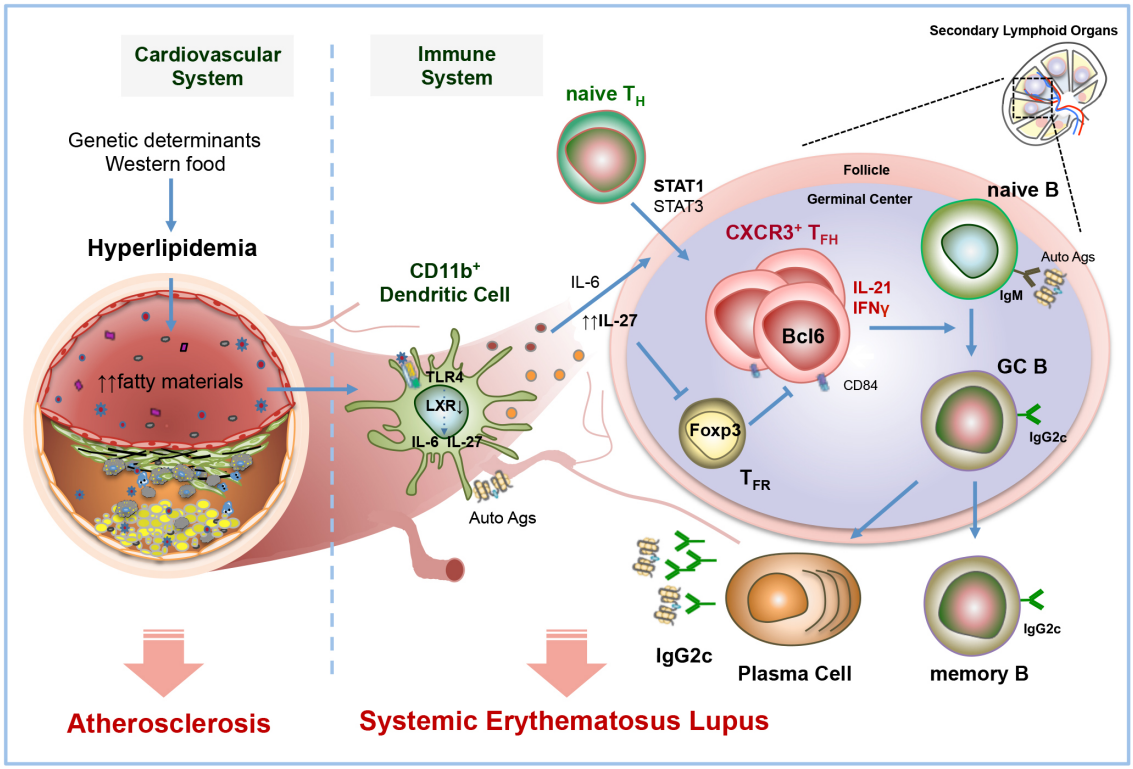

Figure 39. *Graphic summary of this study*[33]

This study demonstrates that atherogenic condition triggers the secretion of IL-27 and IL-6 from CD11b$^+$ dendritic cells in a TLR4-dependent manner. IL-27 activates STAT1 and STAT3 signaling pathway in T cells and increases the numbers of CXCR3$^+$ T_{FH} cells while suppressing T_{FR} cells. These CXCR3$^+$ T_{FH} cells, in turn, stimulate the differentiation of autoreactive B cells into IgG2c-secreting plasma cells, and pathogenic IgG2c autoantibodies exacerbate autoimmune lupus. Thus, hyperlipidemia not only induces cardiovascular diseases but also promotes autoimmune lupus.

production, and (iii) IL-27, but not IL-6, was increased in patients with hypercholesterolemia. Unexpected finding is that blockade of IL-27 signal in both hyperlipidemic and physiological conditions promote T_{FR} cells generation, which are responsible for controlling germinal center reactions. Further studies are necessary how IL-27 regulates T_{FR} generation.

2. IgG2c regulation by CXCR3$^+$ T_{FH} cell

Administration of IL-27 to CXCR3$^-$ T_{FH} cells induced CXCR3 expression in vitro, and deletion of IL-27EBI3 in hyperlipidemic condition almost completely reduced the increased production of IgG2c and the generation of CXCR3$^+$ T_{FH} cells to the levels of

WT mice. Previously, generation of IgG2c is mediated by either IFN-γ production by $CXCR3^+$ T_{FH} cells or T_H1 cells. T_H1 cells have been recently shown to mediate the generation of low affinity neutralizing antibodies in the absence of T_{FH} cells in a viral infection model.

Despite the contribution of T_H1 cells to the increased antibody production in atherogenic mice is not negligible[35], T_{FH} cells isolated from the atherogenic mice were far potent in stimulating IgG2c production from B cells than non-T_{FH} cells. Also, disrupting T-B cell interaction by anti-ICOS administration lead significant reduction of antibody production in vivo, strongly suggesting that T_{FH} cells play a major role in the enhanced antibody production in atherogenic mice.

IgG2 subclasses are more pathogenic in autoimmunity than IgG1 or IgG3 in mice due to their ability to activate the complement pathway and to bind to activating Fc receptors[27]. In this regard, it is noteworthy that patients with hypercholesterolemia exhibited higher levels of IgG1 and IgG3, suggesting that atherogenic dyslipidemia might also promote the production of IgG1 and IgG3 via IL-27 in humans.

3. Role of LXR during pathogenesis of atherosclerosis and SLE

Increasing numbers of studies suggest that pathogenesis of atherosclerosis of mediated by both metabolic factors, such as LDL, and immune cells. Activated immune cells are infiltrated into mature and complex plaques and become prone to rupture and thrombosis[36]. T_H1 and T_H17 subsets of helper T cells are found in the lesion; T_H1 cells seem to be proatherogenic, whereas the role of T_H17 cells remains controversial[10, 37]. Recently T_{FH} and T_{FR} cells are also localized in the lesion, and serve as atherogenic and atheroprotective role, respectively[38]. LXR is a nuclear receptor that senses cholesterol metabolites to regulate its target genes related to cholesterol transport, cholesterol conversion, and intestinal cholesterol absorption. Studies in various models have shown the potential therapeutic efficacy of targeting LXR to cure atherosclerosis. Administration of synthetic LXR agonist, GW3965, to atherosclerosis-prone mice (*Apoe*$^{-/-}$ and *Ldlr*$^{-/-}$ mice) ameliorates lesion development by inhibition of IL-6, IL-1β, and iNOS production by macrophages[20]. Also, LXR activation in human $CD4^+$ T cells

negatively regulates proinflammatory cytokines such as IFN-γ, TNF-α, IL-2, while increases IL-10 production[39].

Meanwhile, SLE is an autoimmune disease mediated by autoantibody production. Some studies suggest that LXR is one of the key factors during pathogenesis of SLE. Since LXR signaling is essential for clearance of apoptotic cells by macrophages[18], deletion of *Nr1h3* (encodes LXRα) and *Nr1h3* (encodes LXRβ) in mice leads development of autoimmune lupus-like phenotypes, such as increase in levels of autoantibodies, deposition of immune complexes. In addition, systemic administration of LXR agonist to lupus-prone mine, $B6^{lpr/lpr}$ mice, ameliorates lupus-like phenotype, such as lymphadenopathy and immune complex deposition in kidney[25].

In the current study, I suggest LXR as a novel therapeutic target for SLE by regulation of IL-27 production by dendritic cells. LXR agonist could downregulate IL-27 production by dendritic cells, which in turns inhibited T_{FH} cell differentiation and consequent germinal center reaction. However, further studies will be needed whether LXR agonist also directly affects other germinal center participants such as T_{FH} cells or B cells.

4. Lipid metabolism and IL-27 production by dendritic cell

Multiple possible mechanisms have been proposed by which atherogenic environment induces IL-27 production from DCs. First of all, fatty material accumulation in atherogenic mice stimulates IL-27 production by the DCs. It has been shown in this study and by others that oxLDL and saturated long-chain fatty acids induce IL-27 production by DCs. Also, TLR4 plays a critical role in the generation of IL-27 under atherogenic condition, suggesting that fatty materials trigger IL-27 production from DCs directly or synergistically with other pathogen-associated molecular patterns (PAMPs) via TLR4.

Secondly, the upregulation in OCR and ECAR observed in DCs from hyperlipidemic condition accounts for highly energy-generating metabolic pathways and might increase IL-27 production, since it has been proposed that energy metabolism significantly impacts cytokine production by DCs.

Most interestingly, it is presumable that downregulation of LXRβ leads IL-27 production by DCs. DCs from the atherogenic mice expressed lower levels of lipid-activated transcription factors, particularly *Nr1h2* (encoding LXRβ), and activation of LXR significantly reduced IL-27 production by the DCs. Also, *Nr1h2*$^{-/-}$ mice exhibited significant elevation in *Ebi3* and *Il27* transcripts. This notion is supported by a recent study showing that LXR-deficient DCs upregulate the production of pro-inflammatory cytokines. Surprisingly, deletion of *Tlr4* did not affect LXR-mediated inhibition of IL-27, suggesting that LXR regulates IL-27 production by DCs in TLR4-independent manner. Altogether, alteration in lipid metabolism including lipid accumulation, energy metabolism, and transcriptional changes, can certainly regulate IL-27 production by DCs generated in hyperlipidemic condition.

5. Clinical implication

An elevated level of IL-27 is found in the atherosclerotic plaques of patients with coronary artery disease. It up regulates ICAM-1 and VCAM-1, IL-6, CCL5, CXCL10 from the artery endothelial cells, leading to the infiltration of inflammatory immune cells into the lesions[30, 40, 41]. The role of IL-27 in lupus is still controversial. IL-27 is positively correlated with the renal SLEDAI[42], and, lack of IL-27 receptor ameliorates the disease severity in a *Sanroque* mice model of lupus[43]. By contrast, administration of IL-27 or enhancing IL-27 signaling ameliorates the severity of lupus in animal model[44]. Our findings support the notion that IL-27 is pathogenic in lupus because it increases T_{FH} cell responses and promotes the production of pathogenic subclasses of IgG in atherogenic environment in vivo. In summary, the present study unveils 'hyperlipidemia-TLR4-IL-27-CXCR3^{+} T_{FH} cell' axis as a novel mechanism by which atherogenic environment promotes GC reactions, which might explain the tight association of atherosclerosis and SLE in humans. Targeting IL-27 therefore might be effective for the treatment of antibody-mediated autoimmune diseases including SLE in patients with hypercholesterolemia (**Figure 42**).

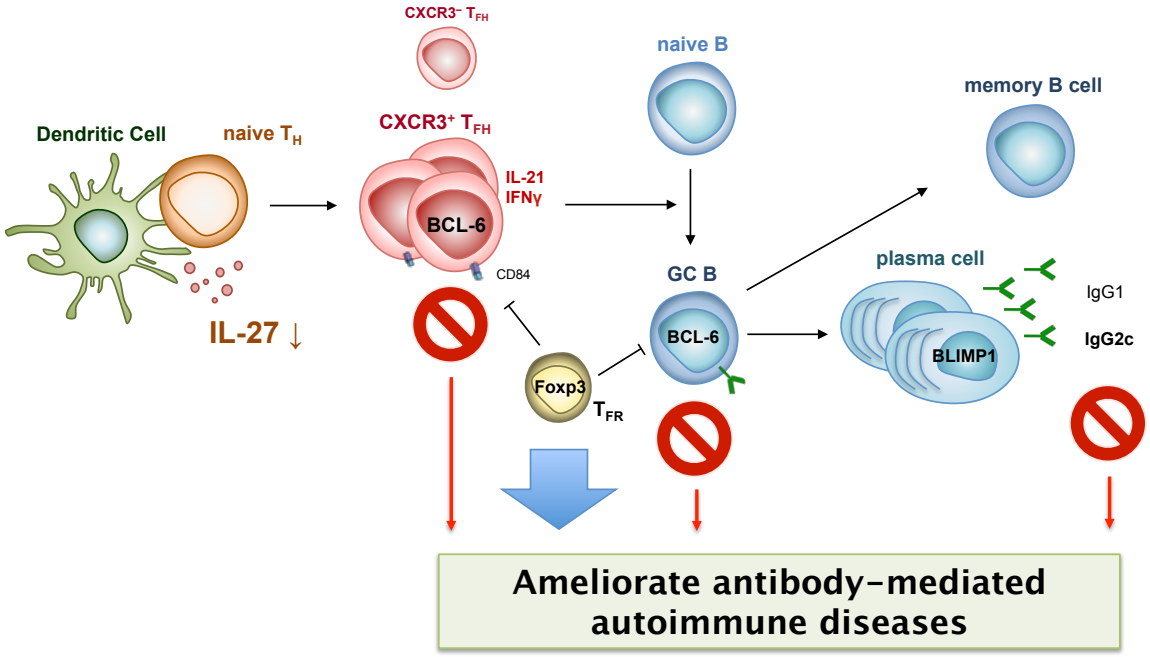

Figure 42. *Clinical implication: Neutralization of IL-27*

Neutralization of IL-27 inhibits generation of $CXCR3^+$ T_{FH} cells and promotes differentiation of T_{FR} cells. These result in decreased production of pathogenic IgG2c antibodies, and ameliorate antibody-mediated autoimmune diseases such as systemic lupus.

Polymorphisms of LXR are found in patients with SLE[45] and LXR-deficiency in mice leads lupus-like phenotypes[21]. LXR promotes phagocytosis by upregulating MERTK expression, which controls self-tolerance and pathogenesis of lupus, and inhibits proinflammatory genes through repression of NF-κB-dependent inflammatory pathways[46]. In the present study, hyperlipidemia, in somehow, lowered LXR expression in dendritic cells to promote secretion of proinflammatory cytokines such as IL-27 and IL-6, and consequent antibody production against self-antigens. Based on these findings, it is plausible that administration of LXR agonist to the patients with antibody-mediated autoimmune diseases, such as SLE, can ameliorate or possibly cure the diseases by inhibiting IL-27 production by dendritic cells and consequent autoantibody production (**Figure 43**).

Notably, hyperlipidemic condition not only promoted production of autoantibodies but also generation of antigen-specific antibodies. It is likely that hyperlipidemic condition lowers antigen susceptibility and tolerance of dendritic cells that might reprogram dendritic cells to generate proinflammatory cytokines more readily

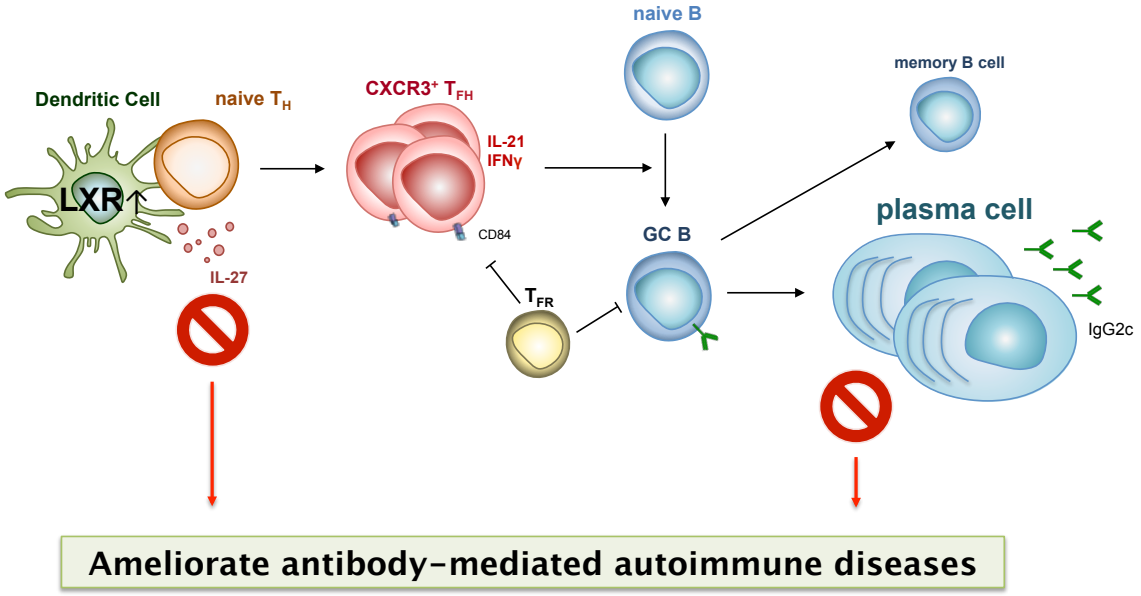

Figure 43. *Clinical implication: LXR agonist*

Administration of LXR agonist inhibits IL-27 production by dendritic cells and consequent autoantibody production, which can ameliorate antibody-mediated autoimmune diseases such as systemic lupus.

regardless of antigen sources. However, further studies are necessary to demonstrate how hyperlipidemia controls antigen susceptibility and immune tolerance of dendritic cells.

Lipid metabolism and immune cells have been thought as a part of independent system. In this study, however, I suggested a new mechanistic insight of pathogenesis of antibody-mediated autoimmune diseases by integration of metabolic disorders and humoral responses. Lipid metabolites or lipid-activated transcription factors regulate antibody-generating germinal center reactions, particular specificity towards pathogenic antibodies or antibody-producing cells. With this foundation of the newly identified mechanism, including IL-27 and LXR, a new therapy for autoimmune diseases can be carefully designed that is effective for antibody-mediated autoimmune diseases, including SLE.

REFERENCES

1. Nurieva, R.I. & Chung, Y. Understanding the development and function of T follicular helper cells. *Cellular And Molecular Immunology* **7**, 190 (2010).

2. Morita, R. *et al.* Human Blood CXCR5+CD4+ T Cells Are Counterparts of T Follicular Cells and Contain Specific Subsets that Differentially Support Antibody Secretion. *Immunity* **34**, 108-121 (2011).

3. Schmitt, N., Bentebibel, S.-E. & Ueno, H. Phenotype and functions of memory Tfh cells in human blood. *Trends Immunol* **35**, 436-442 (2014).

4. Crotty, S. Follicular Helper CD4 T Cells (TFH). *Annual Review of Immunology* **29**, 621-663 (2011).

5. De Silva, N.S. & Klein, U. Dynamics of B cells in germinal centres. *Nature Reviews Immunology* **15**, 137 (2015).

6. Pons-Estel, G.J., Alarcon Gs Fau - Scofield, L., Scofield L Fau - Reinlib, L., Reinlib L Fau - Cooper, G.S. & Cooper, G.S. Understanding the epidemiology and progression of systemic lupus erythematosus.

7. Tsokos, G.C., Lo, M.S., Reis, P.C. & Sullivan, K.E. New insights into the immunopathogenesis of systemic lupus erythematosus. *Nature Reviews Rheumatology* **12**, 716 (2016).

8. Mok, C.C. & Lau, C.S. Pathogenesis of systemic lupus erythematosus. *Journal of Clinical Pathology* **56**, 481 (2003).

9. Vukelic, M., Li, Y. & Kyttaris, V.C. Novel Treatments in Lupus. *Frontiers in Immunology* **9** (2018).

10. Goodson, N., Marks, J., Lunt, M. & Symmons, D. Cardiovascular admissions and mortality in an inception cohort of patients with rheumatoid arthritis with onset in the 1980s and 1990s. *Annals of the Rheumatic Diseases* **64**, 1595-1601 (2005).

11. Kimball, A.B. *et al.* Cardiovascular Disease and Risk Factors among Psoriasis Patients in Two US Healthcare Databases, 2001–2002. *Dermatology* **217**, 27-37 (2008).

12. Roman, M.J. *et al.* Prevalence and Correlates of Accelerated Atherosclerosis in Systemic Lupus Erythematosus. *New England Journal of Medicine* **349**, 2399-2406 (2003).

13. Yu, H.-H. *et al.* Statin reduces mortality and morbidity in systemic lupus erythematosus patients with hyperlipidemia: A nationwide population-based cohort study. *Atherosclerosis* **243**, 11-18 (2015).

14. Ghazizadeh, R., Tosa, M. & Ghazizadeh, M. Clinical Improvement in Psoriasis With Treatment of Associated Hyperlipidemia. *The American Journal of the Medical Sciences* **341**, 394-398 (2011).

15. Choi, J.Y. *et al.* Circulating follicular helper-like T cells in systemic lupus erythematosus: association with disease activity.

16. McDonald G Fau - Deepak, S. *et al.* Normalizing glycosphingolipids restores function in CD4+ T cells from lupus patients.

17. Yuan, J., Li, L.I., Wang, Z., Song, W. & Zhang, Z. Dyslipidemia in patients with systemic lupus erythematosus: Association with disease activity and B-type natriuretic peptide levels. (2016).

18. Kiss, M., Czimmerer, Z. & Nagy, L. The role of lipid-activated nuclear receptors in shaping macrophage and dendritic cell function: From physiology to pathology. *Journal of Allergy and Clinical Immunology* **132**, 264-286 (2013).

19. Schulman, I.G. Liver X receptors link lipid metabolism and inflammation. (2017).

20. Calkin, A.C. & Tontonoz, P. Liver x receptor signaling pathways and atherosclerosis. *Arteriosclerosis, thrombosis, and vascular biology* **30**, 1513-1518 (2010).

21. Westerterp, M. *et al.* Cholesterol Accumulation in Dendritic Cells Links the Inflammasome to Acquired Immunity. (2017).

22. Solt, L.A., Kamenecka, T.M. & Burris, T.P. LXR-Mediated Inhibition of CD4+ T Helper Cells. *PLOS ONE* **7**, e46615 (2012).

23. Herold, M. *et al.* Liver X receptor activation promotes differentiation of regulatory T cells. *PLOS ONE* **12**, e0184985 (2017).

24. Park, H.-J. *et al.* PPARγ Negatively Regulates T Cell Activation to Prevent Follicular Helper T Cells and Germinal Center Formation. *PLOS ONE* **9**, e99127 (2014).

25. A-Gonzalez, N. *et al.* Apoptotic Cells Promote Their Own Clearance and Immune Tolerance through Activation of the Nuclear Receptor LXR. *Immunity* **31**, 245-258 (2009).

26. Kim, Y.U., Lim, H., Jung, H.E., Wetsel, R.A. & Chung, Y. Regulation of Autoimmune Germinal Center Reactions in Lupus-Prone BXD2 Mice by Follicular Helper T Cells. *PLOS ONE* **10**, e0120294 (2015).

27. Baudino, L., Azeredo da Silveira, S., Nakata, M. & Izui, S. Molecular and cellular basis for pathogenicity of autoantibodies: lessons from murine monoclonal autoantibodies. *Springer Seminars in Immunopathology* **28**, 175-184 (2006).

28. Batten, M. *et al.* IL-27 supports germinal center function by enhancing IL-21 production and the function of T follicular helper cells. *The Journal of Experimental Medicine* **207**, 2895 (2010).

29. Shortman, K. & Liu, Y.-J. Mouse and human dendritic cell subtypes. *Nat Rev Immunol* **2**, 151-161 (2002).

30. Lim, H. *et al.* Proatherogenic Conditions Promote Autoimmune T Helper 17 Cell Responses In Vivo. *Immunity* **40**, 153-165 (2014).

31. Reynolds, C.M. *et al.* Dietary saturated fatty acids prime the NLRP3 inflammasome via TLR4 in dendritic cells—implications for diet-induced insulin resistance. *Molecular Nutrition & Food Research* **56**, 1212-1222 (2012).

32. Stumhofer, J.S. *et al.* Interleukins 27 and 6 induce STAT3-mediated T cell production of interleukin 10. *Nat Immunol* **12** (2007).

33. Snapper, C.M. *et al.* Induction of IgG3 secretion by interferon gamma: a model for T cell-independent class switching in response to T cell-independent type 2 antigens. *The Journal of Experimental Medicine* **175**, 1367 (1992).

34. Ryu, H. *et al.* Atherogenic dyslipidemia promotes autoimmune follicular helper T cell responses via IL-27. *Nature Immunology* **19**, 583-593 (2018).

35. Miyauchi, K. *et al.* Protective neutralizing influenza antibody response in the absence of T follicular helper cells. *Nature Immunology* **17**, 1447 (2016).

36. Hansson, G.K. & Libby, P. The immune response in atherosclerosis: a double-edged sword. *Nat Rev Immunol* **6**, 508-519 (2006).

37. Danzaki, K. *et al.* Interleukin-17A Deficiency Accelerates Unstable Atherosclerotic Plaque Formation in Apolipoprotein E-Deficient Mice. *Arteriosclerosis, Thrombosis, and Vascular Biology* **32**, 273 (2012).

38. Baptista, D., Mach, F. & Brandt, K.J. Follicular regulatory T cell in atherosclerosis. *J Leukoc Biol* **104**, 925-930 (2018).

39. Walcher, D. *et al.* LXR Activation Reduces Proinflammatory Cytokine Expression in Human CD4-Positive Lymphocytes. *Arteriosclerosis, Thrombosis, and Vascular Biology* **26**, 1022-1028 (2006).

40. Dorosz, S.A. *et al.* Role of Calprotectin as a Modulator of the IL27-Mediated Proinflammatory Effect on Endothelial Cells. *Mediators of Inflammation* **2015**, 16 (2015).

41. Qiu, H.-N., Liu, B., Liu, W. & Liu, S. Interleukin-27 enhances TNF-α-mediated activation of human coronary artery endothelial cells. *Molecular and Cellular Biochemistry* **411**, 1-10 (2016).

42. Xia, L.P., Li, B.F., Shen, H. & Lu, J. Interleukin-27 and interleukin-23 in patients with systemic lupus erythematosus: possible role in lupus nephritis. *Scandinavian Journal of Rheumatology* **44**, 200-205 (2015).

43. Vijayan, D. *et al.* IL-27 Directly Enhances Germinal Center B Cell Activity and Potentiates Lupus in *Sanroque* Mice. *The Journal of Immunology* **197**, 3008 (2016).

44. Pan, H.-F., Tao, J.-H. & Ye, D.-Q. Therapeutic potential of IL-27 in systemic lupus erythematosus. *Expert Opinion on Therapeutic Targets* **14**, 479-484 (2010).

45. Jeon, J.-Y. *et al.* Liver X receptors alpha gene (NR1H3) promoter polymorphisms are associated with systemic lupus erythematosus in Koreans. *Arthritis Res Ther* **16**, R112-R112 (2014).

46. Kidani, Y. & Bensinger, S.J. Liver X receptor and peroxisome proliferator-activated receptor as integrators of lipid homeostasis and immunity. *Immunol Rev* **249**, 72-83 (2012).

국문 초록

자가면역 질환 환자에서 동맥경화 발병률이 증가되어 있음이 알려져있다. 하지만 고지혈 환경이 어떠한 기전으로 자가면역질환을 조절하는지에 대해 보고되지 않았다. 자가면역질환이 helper T 세포, 특히 T_{FH} 세포 (T follicular helper cell),와 자가항체 (autoantibody)에 의해 매개되는 것이 알려져 있기때문에, 고지혈 환경 유발 인자, 예를 들면 지방대사체와 지방 활성 전사인자 (transcription factor) 등이 항체 생성과 항체 생성을 담당하는 배중심반응 (germinal center reaction)에 어떠한 영향을 주는지 확인하였다.

루푸스 질환 마우스 모델인 BXD2 마우스의 골수세포를 동맥경화 마우스 모델인 *Apoe*$^{-/-}$ 마우스에 이식하였을 때, 자가항체 생성 및 사구체신염 증상이 야생형 마우스 대비 증가하여있음을 확인하였다. 또한 증가된 항체생성은 CXCR3^{+} T_{FH} 세포와 정적 상관관계를 보였으며, *Apoe*$^{-/-}$ 마우스에서 분리한 T_{FH} 세포는 항체 생성 유발 능력이 뛰어난 것으로 확인되었다.

고지혈 환경에서 증가 되어있는 지질체들이 Toll-like receptor 4 (TLR4)와 Liver X receptor (LXR)의 조절을 통하여 수지상세포 (dendritic cell, DC)에 의해서 생성되는 염증성 사이토카인 IL-27 의 생성을 조절한다. 특히 고지혈 환경에서 Interleukine-27 (IL-27)의 양을 증가되어 있음을 마우스모델을 통해 확인하였다. 증가한 IL-27 은 STAT1 과 STAT3 신호전달을 통하여, T_{FH} 세포, 특히 CXCR3 를 발현하는 T_{FH} 아형을 증가시켜, B 세포로 하여금 루푸스에 병원성 항체인 IgG2c 의 생성을 촉진시킨다.

본 연구를 통하여 고지혈 환경 유발 인자, 특히 LXR 전사인자의 작용을 통해, 자가면역질환에 중요한 항체생성반응이 조절됨을 확인하였다. 현재까지 면역질환에서 시도되고 있지 않은 고지혈 환경 유발 인자를 활용한 혁신적인 치료 방법 및 신약 표적을 제시하였다.

주요어

고지혈, 자가면역질환, 여포보조 T 세포 (follicular helper T cell), 배중심반응 (germinal center reaction), IL-27

ACKNOWLEDGEMENT

초등학교 6 년 이후 가장 오랜 시간을 보냈던 박사학위 과정을 마치는 순간이 왔습니다. 모든 것을 다 포기할까 고민하던 순간들이 많았습니다. 실제로 많은 어려움과 흔들림이 있었습니다. 그 과정들을 극복하면서 학위를 받기까지 많은 분들의 지지와 도움이 있었기에, 감사의 인사를 드리고자 합니다.

학문적으로, 또는 정신적으로 많은 지지와 도움을 주신 저의 지도 교수님, 정연석 교수님께 제일 먼저 감사드립니다. 다홍색 치마를 입고 처음 교수님을 뵙던 날을 아직 기억합니다. 면역학에 대한 지식은 물론 생물학적인 기초 지식도 거의 없던 저를 믿고 뽑아 주셨습니다. 학위를 마칠 때 쯤에는 교수님의 기대치에 100% 부응 하는 제자가 되고 싶었으나 늘 부족한 모습만 보여드렸습니다. 발표 후 acknowledgment 를 할 수 있는 시간이 있으면, 항상 저의 교수님에 대한 수식 어구는 '끊임없는 지지와 인내로 지도하여 주시는 존경하는 교수님'이라는 말이었습니다. 처음 입학 때부터 지금 이 순간까지 학문적으로, 또는 한 사람의 인간으로 교수님의 지도 덕분에 (조금은) 성장할 수 있었습니다. 감사합니다.

학위 논문 심사위원장을 맡아주신 서울대학교 약학대학 강창율 교수님, 부위원장을 맡아주신 서울대학교 약학대학 이미옥 교수님, 위원을 맡아주신 한양대학교 의과대학 윤지희 교수님, 서울대학교 의과대학 최윤수 교수님께 감사드립니다. 바쁘신 와중에 좋은 의견과 제안을 해주셔서 학위논문을 마무리 할 수 있었습니다. 더 좋은 연구자로 성장하겠습니다. 감사합니다.

5 년을 함께한 실험실 분들께 감사드립니다. 본 학위 논문의 선행연구를 진행해 주셨던 임호용 박사님 감사합니다. 처음 입학하여 마우스 보정하는 법도 몰랐던 저를 가르쳐 주셔서 졸업을 할 수 있게 되었습니다. 감사합니다. 생각하지 못했던 여러 실험적 아이디어를 알려주신 김병석 박사님, 첫인상은 어려워 보였지만 늘 젠틀하신 박영준 박사님, 옆에서 응원해주신 실험 능력자 조민경 박사님 감사합니다. 힘들 때 의지가 되어준 모든 일을 열심히 하는 최가람 언니, 언제쯤 밥 같이 먹을까 입학 동기 나형진, 늘 웃는 얼굴과 긍정적인 모습을 닮고 싶은 이련 언니, 실험실 무한 에너자이저 활력소 권다솔, 사고뭉치 언니랑 실험한다고 많이 힘들었을 김지연, 열심히 배우자 실험실 막내 김대홍, 행정일 담당 해주셨던 신주희 선생님 포함 모든 실험실 멤버 분들께 감사드립니다.

나의 베스트 술메이트이자 점심메이트인 육식성애자 송성미 언니, 차분하지만 어디선가 누군가에 무슨일이 생기면 나타나는 안선호. 힘들 때면 인천 대구에서 바로 달려와 큰 의지와 힘이 되어주는 오랜 친구 탁희연, 김영화. 다들 많이 보고싶고, 있는 그대로의 나와 함께해줘서 고맙습니다.

29 년 동안 부족한 딸, 한결같이 지지하고 사랑해주신 부모님께 감사드립니다. '음악 전공하겠다, 유학가겠다, 대학원 갈 것이다' 뭐든 자기 멋대로, 하고 싶은 대로 행동했던 딸이었습니다. 돌고 돌아서 드디어 하고 싶은 것을 찾았을 때, 큰 좌절들이 있었습니다. 많은 상처를 드렸습니다. 그러한 상황 속에서도 끝까지 제 판단과 선택을 믿어주시고 최선을 다해서 지지하고 응원해주셔서 감사합니다. 표현도 잘 못하고 무뚝뚝한 딸이지만, 항상 존경하고 사랑합니다. 곁에서 항상 응원하고 지켜주신 외삼촌, 외할머니 감사합니다. 마지막으로 사랑하는 우리 딸 채원이. 우리 채원이가 빨리 커서 이 글을 읽을 수 있었으면 좋겠네. 바쁘다는 핑계로, 피곤하다는 핑계로 놀아주지 못하고 옆에 함께하지 못해서 미안해. 채원이가 엄마를 이해하고 용서 해주길 바란다. 엄마 딸 해줘서 고맙고, 많이 사랑해.

이 외에도 많은 분들의 도움과 보살핌으로 학위를 잘 마칠 수 있었습니다. 다시 한 번 모든 분들께 감사드리며, 훌륭한 과학자로, 연구자로, 한 사람의 인간으로 잘 성장할 수 있도록 노력하겠습니다.